



บัณฑิตวิทยาลัย จุฬาลงกรณ์มหาวิทยาลัย
Graduate School, Chulalongkorn University
เสาหลักของแผ่นดิน

การกักเก็บคลื่นความชื้นในไมโครสเฟียร์แอลจินเนต-ไคโทซานโดยอิเล็กโทรสเปรย์

นางสาวอรอุมา ทิมุลนีย์

วิทยานิพนธ์นี้เป็นส่วนหนึ่งของการศึกษาตามหลักสูตรปริญญาวิทยาศาสตรมหาบัณฑิต
สาขาวิชาปิโตรเคมีและวิทยาศาสตร์พอลิเมอร์
คณะวิทยาศาสตร์ จุฬาลงกรณ์มหาวิทยาลัย
ปีการศึกษา 2552
ลิขสิทธิ์ของจุฬาลงกรณ์มหาวิทยาลัย



บัณฑิตวิทยาลัย จุฬาลงกรณ์มหาวิทยาลัย
Graduate School , Chulalongkorn University
เสาหลักของแผ่นดิน

ENCAPSULATION OF CLINDAMYCIN IN ALGINATE-CHITOSAN
MICROSPHERES BY ELECTROSPRAY

Miss Ornuma Thimulnee

A Thesis Submitted in Partial Fulfillment of the Requirements
for the Degree of Master of Science Program in Petrochemistry and Polymer Science
Faculty of Science
Chulalongkorn University
Academic Year 2009
Copyright of Chulalongkorn University



อรอุมา ทิมุลนีย์: การกักเก็บคลินดามัยซินในไมโครสเฟียร์แอลจินต-ไคโทซานโดยอิเล็กโตรสเปร์รี่ (ENCAPSULATION OF CLINDAMYCIN IN ALGINATE-CHITOSAN MICROSPHERES BY ELECTROSPRAY) อ. ที่ปรึกษาวิทยานิพนธ์หลัก: รศ.ดร.นงนุช เหมือนสิน, อ. ที่ปรึกษาวิทยานิพนธ์ร่วม: ดร.กฤษณา ศิริเลิศมุกุล, 85 หน้า.

ในงานวิจัยนี้ได้เตรียมอนุภาคแอลจินต/ไคโทซานนาโนสเฟียร์โดยใช้เทคนิคอิเล็กโตรสเปร์รี่ โดยศึกษาปัจจัยที่มีผลต่อขนาดและการกระจายขนาดอนุภาค ได้แก่ ศักย์ไฟฟ้า อัตราการไหลของพอลิเมอร์เมื่อออกจากเข็ม เบอร์เข็ม และระยะทางจากปลายเข็มถึงผิวหน้าของสาร ผลการทดลองพบว่า เมื่อเพิ่มศักย์ไฟฟ้าและเบอร์เข็มพบว่าอนุภาคที่ได้มีขนาดเล็กลง แต่เมื่อเพิ่มอัตราการไหลของพอลิเมอร์เมื่อออกจากเข็มและระยะทางจากปลายเข็มถึงผิวหน้าของสารพบว่าอนุภาคที่ได้มีขนาดใหญ่ขึ้น สภาวะที่เหมาะสมที่ใช้ในการเตรียมคลินดามัยซิน-แอลจินต/ไคโทซานคือ ศักย์ไฟฟ้า 15 กิโลโวลต์ อัตราการไหลของพอลิเมอร์เมื่อออกจากเข็ม 10 มิลลิลิตรต่อชั่วโมง เข็มเบอร์ 26 และระยะทางจากปลายเข็มถึงผิวหน้าของสาร 8 เซนติเมตร ขนาดอนุภาคที่ได้เท่ากับ 855 นาโนเมตร อนุภาคที่ได้มีลักษณะเป็นทรงกลมที่มีผิวค่อนข้างเรียบ นอกจากนี้ยังพบว่าขนาดของอนุภาคเพิ่มขึ้นแต่ไม่มีนัยสำคัญเมื่อปริมาณภายในเพิ่มขึ้น จากการศึกษาสามารถกักเก็บยาได้สูงถึง 83% การศึกษาการปลดปล่อยคลินดามัยซินจากอนุภาคแอลจินต/ไคโทซานในฟอสเฟตบัฟเฟอร์พีเอช 7.4 ที่ 37 องศาเซลเซียส พบว่ามีการปลดปล่อยได้สูง 70.35% ภายใน 12 ชั่วโมง และจากการศึกษาเลียนภาวะการแพร่ผ่านผิวหนังของคลินดามัยซินที่ปลดปล่อยออกมาจากอนุภาคแอลจินต/ไคโทซานโดยใช้เมมเบรนเซลลูโลส พบว่ามีคลินดามัยซินปลดปล่อยออกมาอย่างต่อเนื่องตลอดช่วงเวลาที่ศึกษานาน 12 ชั่วโมง นอกจากนี้ยังพบว่าอนุภาคแอลจินต/ไคโทซานที่ได้ยังสามารถยับยั้งเชื้อ *Staphylococcus aureus* ได้อีกด้วย

สาขาวิชา ปิโตรเคมีและวิทยาศาสตร์พอลิเมอร์ ลายมือชื่อนิสิต.....
ปีการศึกษา 2552 ลายมือชื่ออ.ที่ปรึกษาวิทยานิพนธ์หลัก.....
ลายมือชื่ออ.ที่ปรึกษาวิทยานิพนธ์ร่วม.....



5072564923: MAJOR PETROCHEMISTRY AND POLYMER SCIENCE

KEYWORD: ALGINATE/CHITOSAN/CLINDAMYCIN/ELECTROSPRAY

ORNUMA THIMULNEE: ENCAPSULATION OF CLINDAMYCIN IN ALGINATE-CHITOSAN MICROSPHERES BY ELECTROSPRAY.
THESIS ADVISOR: ASSOC. PROF. NONGNUJ MUANGSIN, PhD,
THESIS CO-ADVISOR: KRISANA SIRALEARTMUKUL, PhD, 85 pp.

This research focused on the production of alginate/chitosan nanospheres by electro spray technique. The parameters affected size and size distribution, such as voltage, flow rate, needle gauge and working distance were investigated. The result showed that increasing voltage and needle gauge resulted in a decrease in the sphere size. Whereas when increasing the flow rate and working distance, the sphere size were increased. The optimum condition for producing the clindamycin-alginate/chitosan nanosphere were as follows: voltage of 15 kV, flow rate of 10 mL/h, needle gauge of 26g and working distance of 8 cm. The average size was 855 nm. The morphology of alginate/chitosan nanospheres were spherical shape with smooth surface. Moreover the spherical size increased but not statistically significant when the drug content in the sphere was increased. Encapsulation efficiency of 83% was successfully achieved and up to 70.35% of clindamycin was released from the nanospheres into phosphate buffer pH 7.4 at 37°C within the period of 12 hours. Finally, a simulated skin permeation study of the clindamycin from alginate/chitosan nanospheres using cellulose membrane demonstrated that clindamycin was continuously released from the spheres for up to 12 hours of study. The clindamycin-alginate/chitosan nanospheres have antibacterial activity on *Staphylococcus aureus*.

Field of Study: Petrochemistry and Polymer Science Student's Signature.....

Academic Year: 2009

Advisor's Signature.....

Co-advisor's Signature.....



ACKNOWLEDGMENTS

The author thanks a number of persons for kindly providing the knowledge of this study. First, I would like to express gratitude and appreciation to my advisor, Associate Professor Dr. Nongnuj Muangsin, and Dr. Krisana Siralertmukul for valuable guidance and suggestions throughout this work.

I wish to express my grateful thank to Associate Professor Dr. Sirirat Kokpol, chairman of thesis committee, Assistant Professor Dr. Varawut Tangpasuthadol, examiner for their valuable advice. I also express my appreciation to Dr. Rangrong Yoksan from Kasetsart University, thesis external committee for her valuable comments and suggestions. I also thanks to Dr. Pranee Lertsutthiwong and Dr. Rattapol Rungupan from the Center of Chitin-Chitosan Biomaterial, Metallurgy and Materials Science Research Institute of Chulalongkorn University for suggestion throughout this work.

Furthermore, the author also thanks the Center of Chitin-Chitosan Biomaterial, Metallurgy and Materials Science Research Institute of Chulalongkorn University for providing the equipment, chemicals, and facilities. I thanks the National Center of Excellence for Petroleum, Petrochemicals, and Advanced Materials (NCE-PPAM), Graduate School from Chulalongkorn University for financial support. I wish to express my grateful thank to Dr. Sirapan Sukontasing, Dr. Jomkwan Merak and Anamika Kanjanabuntang from Kasetsart University for assistant about antibacterial test.

Finally, I would like to express my honest thanks to my friend, my family, and especially my parents and brother for their help, cheerful, endless love, understanding and encouragement.

CONTENTS

	PAGE
ABSTRACT (IN THAI).....	iv
ABSTRACT (IN ENGLISH).....	v
ACKNOWLEDGEMENTS.....	vi
CONTENTS.....	vii
LIST OF TABLES	xi
LIST OF FIGURES	xii
LIST OF ABBREVIATIONS.....	xv
CHAPTER I INTRODUCTION.....	1
1.1 Introduction.....	1
1.2 Objectives	3
1.3 Scope and work.....	4
CHAPTER II THEORY AND LITERATURE REVIEW.....	5
2.1 Polymer in pharmaceutical field.....	5
2.2 Alginate.....	5
2.2.1 Alginate uses.....	6
2.3 Chitosan.....	8
2.3.1 Chitosan uses.....	8
2.4 Hydrogel.....	10
2.4.1 Ionotropic and polyelectrolyte complex (PEC) hydrogel.....	10

	PAGE
2.5 Clindamycin.....	11
2.5.1 Physicochemical properties.....	11
2.6 Electro spraying.....	13
2.7 Controlled release system.....	15
2.8 Transdermal delivery systems.....	17
2.9 Franz's cell apparatus	18
2.10 Skin sources.....	19
CHAPTER III EXPERIMENTAL.....	21
3.1 Materials.....	21
3.1.1 Model drugs.....	21
3.1.2 Polymers and chemicals.....	21
3.2 Instruments.....	22
3.3 Nanospheres preparation.....	23
3.3.1 Alginate/chitosan nanospheres preparation.....	23
3.4 Characterization of nanospheres.....	24
3.4.1 Microscopic analysis	24
3.4.2 Particle size measurement.....	24
3.4.3 Zeta potential.....	25
3.4.4 Functional group analysis (FTIR).....	25
3.4.5 Powder x-ray diffraction study (XRD).....	25
3.4.6 Thermal analysis (DSC).....	25
3.5 Determination of drug content and encapsulation efficiency (EE).....	26

	PAGE
3.5.1 Calibration curve of clindamycin in distilled water.....	26
3.5.2 Calibration curve of clindamycin in buffer solution.....	27
3.6 <i>In vitro</i> clindamycin release from clindamycin- loaded alginate/chitosan nanospheres.....	28
3.6.1 Preparation of buffer medium for drug release study.....	28
3.6.2 <i>In vitro</i> drug release.....	28
3.7 <i>In vitro</i> study of drug permeation through cellulose membrane.....	29
3.7.1 Drug permeation studies.....	29
3.7.2 Buffer medium preparation.....	31
3.7.3 Pretreatment of cellulose membrane	31
3.8 Antibacterial Activity of drug loaded ALG/CS-NSs.....	31
3.9 Statistical analysis.....	32
CHAPTER IV RESULTS AND DISCUSSION.....	33
4.1 Synthesis and optimization of fabrication parameter	33
4.2 Characterization of nanospheres.....	41
4.2.1 Morphology.....	41
4.2.2 Fourier transform infrared spectroscopy (FTIR).....	43
4.2.3 Powder x-ray diffraction (XRD).....	47
4.2.4 Differential scanning calorimetry (DSC).....	49
4.3 Evaluation of drug content and drug entrapment efficiency.....	52

	PAGE
4.4 Drug release study of CM-ALG/CS-NSs in phosphate buffer medium.....	53
4.5 <i>In vitro</i> study of clindamycin permeation through cellulose membrane.....	55
4.6 Antibacterial activity of CM-ALG/CS-NSs.....	57
CHAPTER V CONCLUSIONS.....	58
REFERENCES.....	59
APPENDICES.....	67
VITAE.....	85

LIST OF TABLES

TABLE	PAGE
2.1 The animal skins that have been used in permeation studies.....	20
3.1 Instruments.....	22
3.2 The parameters studied for the nanospheres preparation.....	23
4.1 Effect of voltage on spherical size of ALG/CS.....	33
4.2 Effect of flow rate on spherical size of ALG/CS.....	35
4.3 Effect of needle gauge on spherical size of ALG/CS.....	36
4.4 Effect of working distance on spherical size of ALG/CS.....	38
4.5 Effect of mass ratio of alginate to clindamycin on spherical size of ALG/CS and zeta potential produced by optimal condition.....	39
4.6 Clindamycin content and encapsulation efficiency (%EE) of the spheres containing different alginate to drug mass ratios.....	52
4.7 Linear relation between amount of drug permeating through one area division of cellulose membrane (Q_p) and time.....	56

LIST OF FIGURES

FIGURE	PAGE
2.1 Copolymer of α -L-guluronic acid and β -D-mannuronic acid.....	5
2.2 Structure of chitin and chitosan.....	8
2.3 The ionotropic and polyelectrolyte complex (PEC) hydrogel.....	10
2.4 Chemical structure of clindamycin hydrochloride.....	11
2.5 The droplet is generated by electrical force.....	13
2.6 Presentation of controlled release system.....	15
2.7 Presentation of diffusion controlled release	16
2.8 Presentation of swelling controlled release.....	16
2.9 Presentation of erosion controlled release-(a) bulk erosion and (b) surface erosion.....	17
2.10 The components of Franz' s cell.....	19
3.1 The components of Franz's cell and instrument set-up for permeation.....	30
4.1 Effect of voltage on size and size distribution measured by particle sizer.	34
4.2 Effect of flow rate on size and size distribution measured by particle sizer.....	35
4.3 Effect of needle gauge on size and size distribution measured by particle sizer.....	37
4.4 Effect of working distance on size and size distribution measured by particle sizer.....	38

FIGURE	PAGE
4.5 Effect of ALG:CM mass ratio on size and size distribution measured by particle sizer.....	39
4.6 Scanning electron micrograph of ALG/CS-NSs without CM (a) at 20000x and (b) at 50000x , ALG/CS-NSs with CM (c) at 10000x (applied voltage 15 kV, flow rate 10 ml/h, needle gauge 26g and working distance 8 cm).....	41
4.7 Scanning electron micrographs of CM-ALG/CS-NSs at ALG : CM ratio of (a) 1:0.5, (b) 1:1, and (c) 1:2 (applied voltage 15 kV, flow rate 10 mL/h, needle gauge 26g and working distance 8 cm).....	42
4.8 FTIR spectra of (a) alginate, (b) chitosan, and (c) ALG/CS-NSs.....	43
4.9 FTIR spectra of (a) clindamycin (b) CM-ALG/CS-NSs (ALG:CM = 1:0.5), (c) CM-ALG/CS-NSs (ALG:CM = 1:1) and (d) CM-ALG/CS-NSs (ALG:CM = 1:2).....	45
4.10 X-ray diffractograms of (a) alginate, (b) chitosan, (c) ALG/CS-NSs (d) Clindamycin and (e) CM-ALG/CS-NSs.....	47
4.11 DSC thermograms of (a) alginate (b) chitosan (c) ALG/CS-NSs.....	49
4.12 DSC thermograms of (a) clindamycin, (b) CM-ALG/CS-NSs (ALG:CM = 1:0.5), (c) CM-ALG/CS-NSs (ALG:CM = 1:1) and (d) CM-ALG/CS-NSs (ALG:CM = 1:2).....	50
4.13 Comparison of cumulative CM release of CM-ALG/CS-NSs having different alginate to drug ratio. Error bars indicate the range of experimental reading obtained (sample number, n = 3).....	53

FIGURE	PAGE
4.14 Comparison of %cumulative CM release of CM-ALG/CS-NSs having different alginate to drug ratio. Error bars indicate the range of experimental reading obtained (sample number, $n = 3$).....	54
4.15 Permeation profiles of drug through cellulose membrane at various alginate to CM ratio.....	56
4.16 Antibacterial activity of (a) clindamycin, (b) ALG/CS, (C) ALG:CM 1:0.5, (d) ALG:CM 1:1, and (e) ALG:CM 1:2.....	57

LIST OF ABBREVIATIONS

ALG :CM	: alginate:clindamycin
APDs	: avalanche photodiode array
CS	: chitosan
CM-ALG/CS-NSs	: clindamycin-alginate/chitosan nanospheres
CM	: clindamycin
Q_p	: cumulative amount of drug permeated through a unit area of cellulose membrane
cm	: centimeter
DSC	: differential scanning calorimetry
%DD	: degree of deacetylation
EE	: encapsulation efficiency
F	: flux
FTIR	: fourier transform infrared spectrophotometry
g	: gauge
h	: hour
kV	: kilovolt
μ g	: microgram
mg	: milligram
mL/h	: milliliter per hour
mL	: milliliter
MW	: molecular weight
nm	: nanometer
%	: percentage
PDI	: polydispersity index
PEC	: polyelectrolyte complex
pH	: power of hydrogen ion or the negative logarithm (base ten)
KBr	: potassium bromide disk

rpm	: round per minute
SEM	: scanning electron microscopy
SD	: standard deviation
t	: time
v/v	: volume/volume
w/w	: weight/weight
w/v	: weight/volume
XRD	: X-ray diffraction

CHAPTER I

INTRODUCTION

1.1 Introduction

Acne vulgaris is a very common skin disease caused by an inflammatory of follicles and sebaceous gland. The first-line treatment for most patients present with mild to moderate acne is via the topical route. Clindamycin is generally considered to be the most effective topical antibiotic for acne [1], but the main disadvantages of using clindamycin are the side effects, i.e. dryness, peeling, redness, diarrhea and the risk of pseudomembranous colitis, resulting from systemic absorption of the drug [2].

The encapsulation of drug into particles can reduce its side effect, according to previous studies, the encapsulation of clindamycin into liposome can reduce its side effects and improve efficiency of the drug, such as appears to give a higher drug concentration at the intended site of action, resulting to enhanced the localized effect [3]. Moreover, using the carboxymethyl chitosan in clindamycin gel can improve the activity against *Propionibacterium acne* that is involved in causing acne [4].

Polyelectrolyte complex (PEC) consist of oppositely charged polymers when they are mixed via electrostatic interactions. Interaction between anionic alginate and cationic chitosan leads to PEC formation and these PECs have potential applications such as drug or gene delivery systems in biomedicine [5].

Alginate is a naturally occurring anionic polymer that is extracted from marine brown algae and consist of linear chains of α -L-guluronic acid (G) and β -D-mannuronic acid (M) residues joined by 1,4-glycosidic linkages. Water-soluble alginate can be form insoluble particles with calcium chloride on a nanometer scale depending on the concentration of sodium alginate and calcium chloride [6]. Moreover, it has been demonstrated that the addition of cationic polymer such as chitosan [7], pectin, [8], ethylcellulose [9], and Eudragit [9-10]. Successful attempts

involving the cross-linking of sodium alginate alone [10–13] can be enhancing the encapsulation efficiency and prolong sustained release of drugs [14].

Chitosan is a natural cationic polymer that is formed by the *N*-deacetylation of chitin, which is a product found in crustacean shells. Chitosan is a linear copolymer that consists of *D*-glucosamine and *N*-acetyl-*D*-glucosamine units linked by β -(1-4)-glycosidic linkages. Its cationic nature allows formation of complexes with negatively charged polymers such as alginate, carrageenan. The alginate-chitosan polyelectrolyte complex that is biocompatibility, non-toxicity and ability to encapsulate many of low molecular drug [15]. Therefore the alginate-chitosan system is suitable for drug delivery system.

Various method for preparation of alginate-chitosan micro/nanoparticles have been reported such as ionotropic gelation [16] and solvent emulsification/internal gelation [17], but the droplet easily agglomerate and coagulate, moreover they gave a wide size distribution. One of the novel techniques for preparation nanoparticles is known as electrohydrodynamic atomization or electrospray, that a method of liquid of atomization by means of electrical forces. The polymer flowing out of the nozzle in the form of droplet when applied high voltage potential forces. Electrospray systems have several advantages over mechanical atomizers such as the droplet size can be range from hundrate micrometers down to several tens of nanometer, the size distribution of the droplets can be nearly monodisperse, droplet generation and droplet size can be controlled by adjust the flow rate and voltage applied [18]. Moreover the droplet produced by electrospraying are highly charged, that prevents their coagulation and agglomeration [19]. Electrospray technique has many applications such as fabrication of inorganic nanoparticles, thin films, and fibers, production of pharmaceutical particles, deposition of nanoparticles and generation of micro/nanoencapsulation [18].

Arya et al. [20] used the electrosprayed for synthesis of chitosan nanospheres for controlled release of ampicilin. The spherical sizes were about 520 nm and the encapsulation efficiency was 80.4%.

Xie and Wang [21] reported the preparation of the microencapsulation of Hepatocytes G2 cell in calcium alginate microbead by electrospray. The droplet size were with in the range of 200 μm - 20 mm and the sizes of microbead depended on the flow rate and voltage.

Sasaki et al. [22] disclosed the preparation of microcapsules by electrostatic atomization. Sodium alginate and calcium chloride were used as a polymer material for a shell formation and crosslink agent, respectively. Carboxymethyl cellulose was used as core solution. The results showed that the microcapsules with alginate shell and core have been obtained successfully and the capsules size can be reduced to 500 μm in diameter.

In this research, electrospray technique has been employed to fabricate of alginate-chitosan nanospheres. The focus was on the influence of fabrication parameters is on the morphology and size of the spheres formed. Then the optimal conditions were chosen for fabrication of clindamycin-loaded alginate-chitosan nanospheres that are appropriate for drug delivery applications.

1.2 Objectives

The overall objective of this research is to explore the use of electrospray technique to produce alginate-chitosan nanospheres as a carrier for controlled release of clindamycin. Effects of experiment setup such as voltage, flow rate, needle gauge and working distance on morphology and size of the nanospheres were studied. The clindamycin release from alginate-chitosan nanospheres was evaluated in simulated skin permeation study using Franz cell.

1.3 Scope and work

1.3.1 Literature review of related works

1.3.2 Preparation of alginate-chitosan nanospheres and clindamycin-loaded alginate-chitosan nanospheres with parameters including voltage, flow rate, needle gauge and working distance

1.3.3 Characterization of obtained nanospheres in terms of morphology, size, zeta potential, chemical analysis, thermal behavior and crystallinity

1.3.4 Evaluation of drug content and drug encapsulation efficiency as a function of preparation parameters; weight ratio of alginate to clindamycin

1.3.5 *In vitro* clindamycin release study from alginate-chitosan nanospheres at various weight ratios of alginate to clindamycin in phosphate buffer

1.3.6 *In vitro* clindamycin release study under simulated skin permeation condition by using cellulose membrane

1.3.7 Testing for antibacterial against *Staphylococcus aureus*

1.3.8 Report preparation of the summarized results

CHAPTER II

BACKGROUND AND LITERATURE REVIEWS

2.1 Polymer in pharmaceutical field

Polymers are becoming increasingly important in the pharmaceutical industry as both drug encapsulants and vehicles of drug carriage in order to either protect an active agent during its passage through the body until its release, or control its release. Carrier technology obtained the drug delivery system by coupling the drug to the carrier polymers in various dosage forms such as beads, microspheres, nanoparticles, liposomes. Those formulations could delay the release of drug and also generate a response in a specific area or organ of the body requiring treatment. Moreover, a target drug, encapsulated in a polymer can be released sustainedly to improve drug therapeutic efficacy and decrease the dosing time and side effect [23].

Naturally occurring polymers are attractive as drug delivery system since they possess the biocompatibility, biodegradability and non-toxicity required for used in human [15].

2.2 Alginate

Alginate is a naturally occurring anionic polymer that is extracted from marine brown algae and consists of linear chains of α -L-guluronic acid (G) and β -D-mannuronic acid (M) residues joined by 1,4-glycosidic linkages (Fig.2.1).

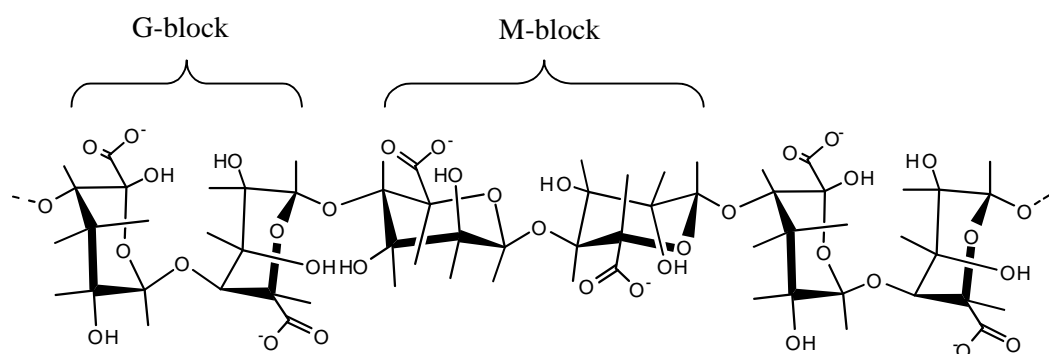


Figure 2.1 Copolymer of α -L-guluronic acid and β -D-mannuronic acid

2.2.1 Alginate uses [24]

The uses of alginates are based on three main properties. The first is their ability to increase the viscosity of aqueous solutions. The second is their ability to form gels; gels form when a calcium salt is added to a solution of sodium alginate in water. The gel forms by chemical reaction, the calcium displaces the sodium from the alginate, holds the long alginate molecules together and a gel is the result. No heat is required and the gels do not melt when heated. The third property of alginates is the ability to form films of sodium or calcium alginate and fibres of calcium alginates. Upon these properties, alginates are widely used in various applications such as textile printing, food and pharmaceutical uses.

1. Textile printing

In textile printing, alginates are used as thickeners for the paste containing the dye. These pastes may be applied to the fabric by either screen or roller printing equipment. Alginates became important thickeners with the advent of reactive dyes. These combine chemically with cellulose in the fabric. Many of the usual thickeners, such as starch, react with the reactive dyes, and this leads to lower colour yields and sometimes by-products that are not easily washed out. Alginates do not react with the dyes, they easily wash out of the finished textile and are the best thickeners for reactive dyes. Textile printing accounts for about 50 percent of the global alginate market.

2. Food

The thickening property of alginate is useful in food product such as sauces, syrups and toppings for ice cream. Addition of alginate can make icings non-sticky and allow the baked goods to be covered with plastic wrap. Alginate can be used as emulsifier in water-in-oil emulsions such as mayonnaise and salad dressings are less likely to separate into their original oil and water phases.

Alginates have some applications that are not related to either their viscosity or gel properties. They act as stabilizers in ice cream by reducing the formation of ice crystals during freezing, giving a smooth product. A variety of agents are used in the

clarification of wine and removal of unwanted coloring, in some cases it has been found that the addition of sodium alginate can be effective.

The gelling properties of alginate were used in the production of artificial cherries since 1946. A flavored and colored solution of sodium alginate was allowed to drop into a solution of calcium salts. Moreover, calcium alginate films and coatings have been used to help to preserve frozen fish. If the fish is frozen in a calcium alginate jelly, the fish is protected from the air and rancidity from oxidation is very limited.

3. Pharmaceutical and medical uses

The fibers of calcium alginate are used in wound dressings. They have very good wound healing and haemostatic properties and can be absorbed by body fluids because the calcium in the fiber is exchanged for sodium from the body fluid to give a soluble sodium alginate. This also makes it easy to remove these dressings from the large open wounds or burns since they do not adhere to the wound. In addition, removal also can be assisted by rinsing the dressing with saline solution to ensure its conversion to soluble sodium alginate.

The good swelling properties of alginic acid powder led to its use as a tablet disintegrant for some specialized applications. Alginic acid has also been used in some dietary foods; it swells in the stomach and gives a full feeling if sufficient amount is taken so the person is dissuaded from further eating.

Alginate is widely used in the controlled release of drugs and other chemicals. In some applications, the active ingredient is placed in a calcium alginate bead and slowly released when the bead is exposed in the appropriate environment.

2.3 Chitosan

Chitosan is a cationic natural linear polysaccharide consisting of copolymers of D-glucosamine and N-acetyl-D-glucosamine units linked by β -(1-4)-glycosidic linkages (Fig. 2.2). It is produced commercially by deacetylation of chitin, which present in outer structure in marine crustaceans such as crabs and shrimp. The degree of deacetylation (%DD) has a significant effect on the solubility and rheological properties of polymer. chitosan is soluble in dilute acidic solution and gives positively charged with a charge density depending on pH and %DA value.

Chitosan is reportedly hydrophilic, nontoxic, biocompatible, and biodegradable. Other properties include adsorption properties and anti-microbial properties. It is therefore considered to be suitable for application in pharmaceutical technology [25].

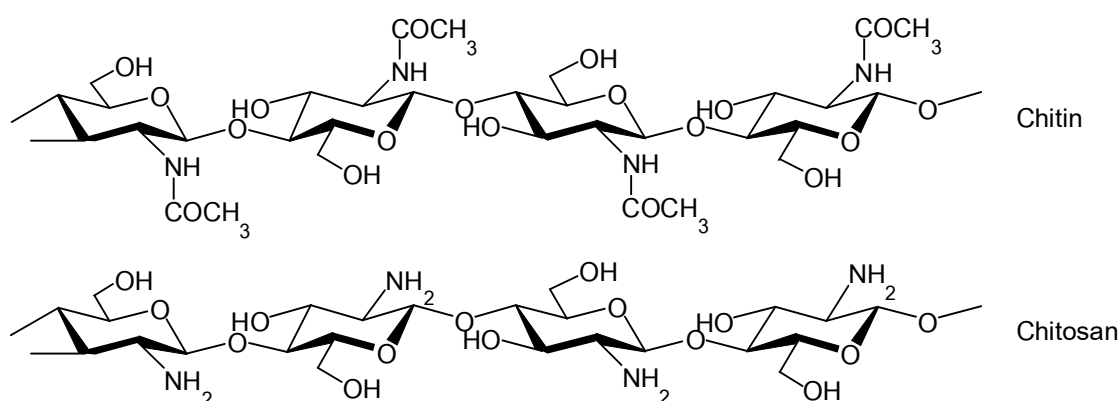


Figure 2.2 Structure of chitin and chitosan

2.3.1 Chitosan uses [26]

1. Cosmetics

Chitosan is a particularly effective hydrating agent which is able to supply water and avoid dehydration. Chitosan form a protective tensor film on the skin's

surface that can fix and allow the active principles to be placed in close contact with the skin. This is a new double advantage that makes chitosan of great interest in cosmetic. Therefore, chitosan are now widely used in skin creams, shampoos, etc.

2. Agriculture

chitosan and its derivatives have plant protecting and antifungal properties. In very low concentration of chitosan, they can stimulate defensive mechanisms in plants against infections and parasite attacks. They can also be used as coatings of seeds which obtained to increase crop yield more than 20% in comparison with uncoated seeds.

3. Water treatment

Chitosan has been gaining interest for industry and nature conservation. They are remarkable as chelating agents and heavy metal traps. The Environmental Protective Agency (EPA) has already approved the use of chitosan in water at concentrations of up to 10 mg per litre. For sewage treatment, chitosan can be used at up to 5 ppm. It reduces the oxygen demand by 80 to 85% and reduces the phosphates level to less than 5 ppm.

4. Pharmaceutical and medical uses

Due to its biocompatibility with human body tissue, chitosan have demonstrated their effectiveness for all forms of dressings – artificial skin, corneal bandages and suture thread in surgery – as well as implants or gum cicatrization in bone repair or dental surgery.

Lastly, chitosan is an excellent medium for carrying and slow release of medicinal active principles in plants, animals and man. The non-antigenic behavior of chitosan promises unlimited development in the health field.

2.4 Hydrogel

Hydrogel is a three-dimension network of polymer chains that are water-insoluble and sometime found as a colloidal gel in which water is the dispersion medium. Hydrogels are superabsorbent which could contain over 99% of water. Hydrogels possess also a degree of flexibility very similar to natural tissue, due to their significant water content.

2.4.1 Ionotropic and polyelectrolyte complex (PEC) hydrogel

Hydrogel formed with oppositely charged multivalent ion is known as an ionotropic hydrogel (Fig. 2.3a) e.g. calcium alginate [27] and calcium pectinate gel [28]. In addition, when the oppositely charged hydrogels are mixed, they give a product of such ion crosslinked systems which are known as complex coacervate or polyelectrolyte complex (PEC) hydrogel (Fig.2.3b). The mixtures of chitosan-alginate and chitosan-carrageenan are the samples of polyelectrolyte complexes [29]. Heidi Vogt et al. reported interactions between cationic chitosan and anionic alginate leads to PEC formation and these PECs have potential applications such as drug or gene delivery system in biomedicine [5].

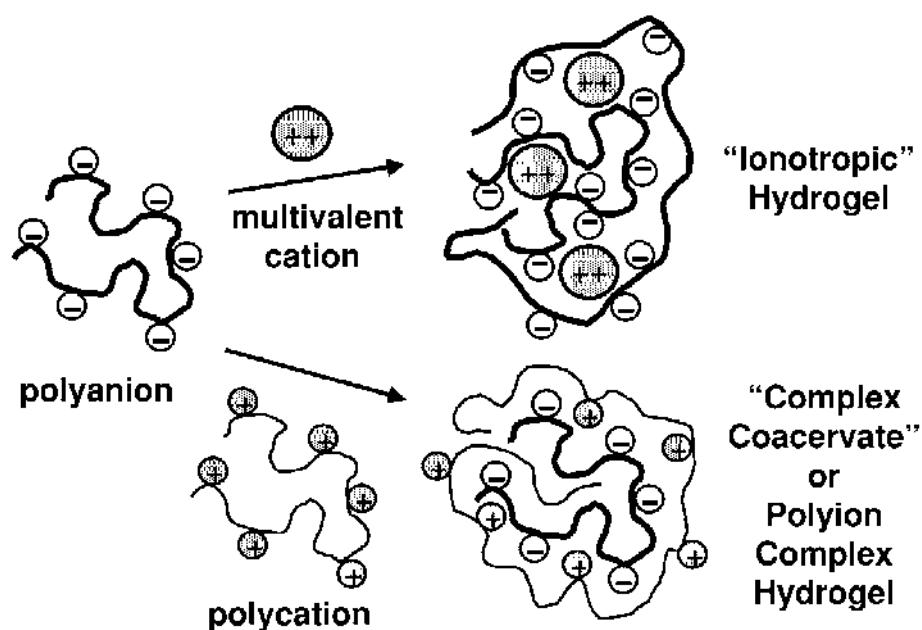


Figure 2.3 The ionotropic and polyelectrolyte complex (PEC) hydrogel [30]

2.5 Clindamycin [31]

Clindamycin is a macrolide antibiotic derived from *Streptomyces lincolnesis*. It exerts its antimicrobial effect by inhibition of bacterial protein synthesis. The drug can be administered topically, orally, or parenterally. It has excellent activity against most staphylococci, group A and B β -hemolytic streptococci, pneumococci, chlamydia, anaerobic organism and *Mycoplasma hominis*. The antibiotic is not effective against aerobic gram-negative bacilli and enterococci [32]. Clindamycin is commonly used for acne treatment.

2.5.1 Physicochemical properties

Clindamycin appears as a white, crystalline powder, very soluble in water and slightly soluble in alcohol.

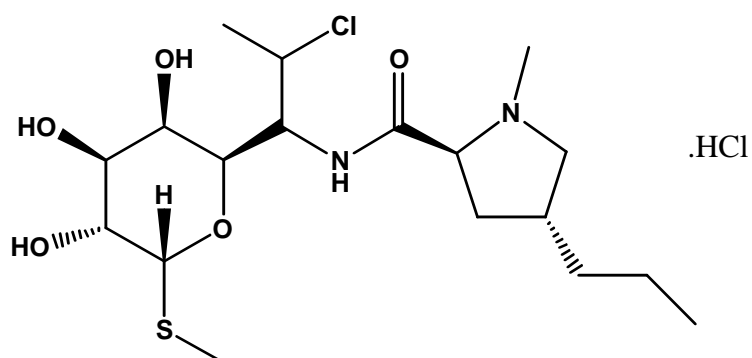


Figure 2.4 Chemical structure of clindamycin hydrochloride

Chemical data

Formula	:	$C_{18}H_{23}ClN_2O_5S$
Molecular weight	:	424.98

IUPAC name	:	(2 <i>S</i> ,4 <i>R</i>)- <i>N</i> -((1 <i>R</i>)-2-chloro-1-((3 <i>R</i> ,4 <i>R</i> ,5 <i>S</i> ,6 <i>R</i>)-3,4,5-trihydroxy-6-(methylthio)-tetrahydro-2 <i>H</i> -pyran-2-yl)propyl)-1-methyl-4-propylpyrrolidine-2-carboxamide
Synonyms	:	7-chloro-lincomycin, 7-chloro-7-deoxylincomycin

Pharmacokinetic data

Bioavailability	:	90% (oral) 4–5% (topical)
Protein binding	:	90%
Metabolism	:	Hepatic
Half life	:	2-3 hour
Excretion	:	Biliary and renal (around 20%)
Route	:	Oral, topical

Susceptible bacteria

It is most effective against infections involving the following types of organisms:

- Aerobic gram-positive cocci, including some members of the *Staphylococcus* and *Streptococcus* (eg. pneumococcus) genera.
- Anaerobic, gram-negative rod-shaped bacteria, including some species of *Bacteroides* and *Fusobacterium*.

Most *aerobic* gram-negative bacteria (such as *Pseudomonas*, *Legionella*, *Haemophilus influenzae* and *Moraxella*), as well as the facultative anaerobic Enterobacteriaceae, are resistant to clindamycin.

Adverse effects

Common adverse drug reactions (ADRs) associated with clindamycin therapy found in over 1% of patients include diarrhea, pseudomembranous colitis, nausea, vomiting, abdominal pain or cramps, rash, and/or itch. High doses (both intravenous and oral) may cause a metallic taste, and topical application may cause contact dermatitis. Pseudomembranous colitis is a potentially-lethal condition commonly associated with clindamycin, but which also occurs with other antibiotics. Overgrowth of *Clostridium difficile*, which is inherently resistant to clindamycin, results in the production of a toxin that causes a range of adverse effects, from diarrhea to colitis and toxic megacolon.

2.6 Electrospray

Electrospray (electrohydrodynamic spraying) is a method of generating a very fine droplet through electrical force (Fig. 2.5). In this process, liquid flowing out from a capillary nozzle maintained at high potential, is subjected to an electric field, which causes elongation of the meniscus to a form of jet or spindle. The jet deforms and disrupts into droplets due mainly to electrical force. In the electro spraying, no additional mechanical energy, other than that from the electric field alone, is needed for liquid atomization [18].

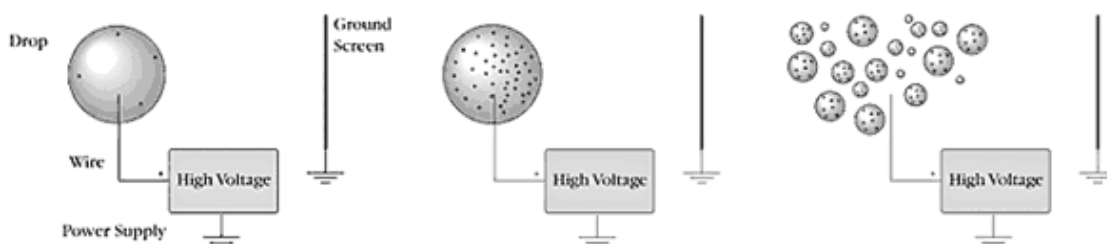


Figure 2.5 The droplet is generated by electrical force

Electrospray allows generation of fine droplets of charge magnitude close to one half of the Rayleigh limit. The Rayleigh limit is the magnitude of charge on a drop that overcomes the surface tension force, that leads to fission of the droplet.

Jaworek reported the charge and size of the droplet can be easily controlled by adjusting the flow rate and voltage applied to the nozzle [19].

Salata [33] have been briefly reviewed about nanoelectrospray technologies that electro-spraying can be widely applied to both industrial processes and scientific instrumentations. The interest in industrial or laboratory applications has recently prompted the search for new, more effective techniques which allow control of the processes in which the droplets are involved. Electrospray is used for micro- and nano-thin-film deposition, micro- or nano-particle production, and micro- or nano-capsule formation. Thin films and fine powders are used in modern material technologies, microelectronics, and medical technology. Research in electro-microencapsulation and electro-emulsification is aimed at developing new drug delivery systems, medicine production, and ingredients dosage in the cosmetics and food industries.

The applications of electro-spraying reviewed by Kruis et al. [34], such as the particles size smaller than 10 μm applied for ceramic coatings, paints, or emulsion production, as powder in the cosmetic or pharmaceutical industries, or as toner in electro-reprographic systems. Nowadays, electro-spray is involved in nanotechnology and nanoelectronics for thin-film deposition [35].

The electro-spraying has some advantages over conventional mechanical spraying systems with droplet charged by induction such as

1. Droplet size is smaller than that available from conventional mechanical atomisers, and can be smaller than 1 μm .
2. The size distribution of the droplets is usually narrow, with small standard deviation that allows production of particles of nearly uniform size.

3. Charged droplets are self-dispersing in space (due to their mutual repulsion), resulting also in the absence of droplet coagulation.

4. The motion of charged droplets can be easily controlled (including deflection or focusing) by electric fields.

5. The deposition efficiency of a charged spray on an object is order of magnitudes higher than for un-charged droplets.

2.7 Controlled release system

The means by which a drug is introduced into the body is almost as important as the drug itself. Drug concentration at the site of action must be maintained at a level that provides maximum therapeutic benefit and minimum toxicity. The pharmaceutical developer must also consider how to transport the drug to the appropriate part of the body and, once there, make it available for use [36].

Controlled drug delivery occurs when a polymer is combined with the drug or other active agents in such a way that the active agent is released from the material in a pre-designed manner.

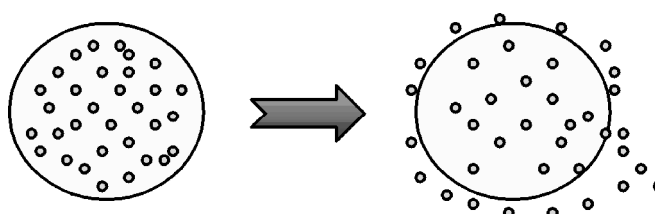


Figure 2.6 Presentation of controlled release system [37]

The drug can be released from the system by 3 mechanisms.

1) *Diffusion Controlled Release*

Diffusion occurs when drug molecules pass from the polymer matrix to the external environment. As the release continues, its rate normally decreases with this type of system, since drug has progressively longer distance to travel and therefore requires a longer diffusion time to release.

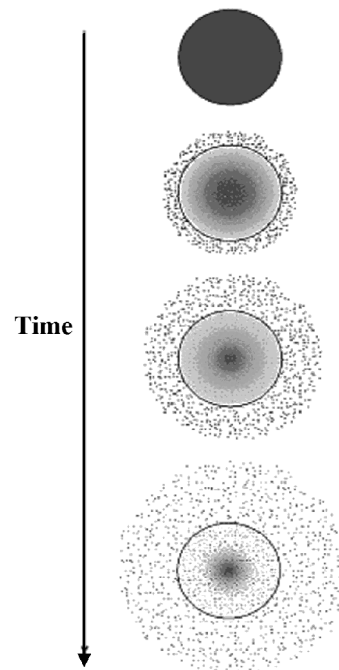


Figure 2.7 Presentation of diffusion controlled release [37]

2) *Swelling Controlled Release*

The swelling of the carrier increases the aqueous solvent content within the polymer matrix, enabling the drug to diffuse through the swollen network into the external environment. Most of materials used are based on hydrogel. The swelling can be triggered by a change in the environment surrounding such as pH, temperature, ionic strength, etc.

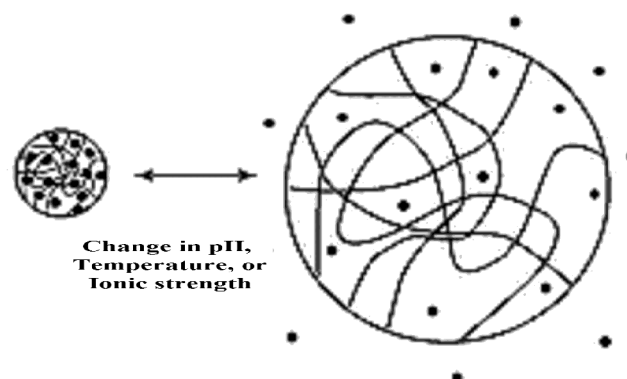


Figure 2.8 Presentation of swelling controlled release [37]

3) *Erosion Controlled Release*

The drug can be released from the matrix due to erosion of polymers, which can be classified into 2 types.

Bulk erosion: The polymer degrades in a fairly uniform manner throughout the polymer matrix.

Surface erosion: The degradation occurs only at the surface of the polymer device.

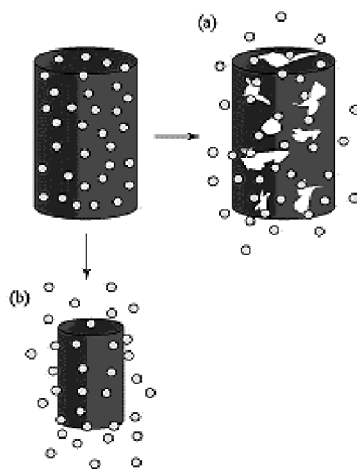


Figure 2.9 Presentation of erosion controlled release-(a) bulk erosion and (b) surface erosion [37]

2.8 Transdermal delivery systems

The skin is an important barrier to controlled drug delivery. Approaches for delivering drugs throughout the skin as well as recent advances in iontophoresis, ultrasound, chemical enhancers, and chemical treatment of drugs for transdermal delivery [38].

Transdermal delivery system is the results of sophisticated procedures, where technology prevailed over a well-known pharmacological component, resulting in the development of the system in a short time. Such development progressed through three stages, or generations, aimed at improving delivery and absorption, reducing patch size and making it easier to use. Furthermore, the therapeutic benefits of transdermal drug delivery systems are an important issue in the development of any drug products.

The advantages transdermal drug delivery are:

- Adaptability to drugs with a short half-life.
- Avoidance of variation in gastrointestinal absorption.
- By pass of the hepatic first pass metabolism.
- Good patient compliance.
- Production of sustained and constant plasma concentrations of drugs
- Reduction in repeated dosing intervals.
- Reduction of potential adverse side effects.
- Removal of transdermal drug delivery systems provokes an immediate decrease of drug plasma levels.
- Substitute for oral or parenteral administration in certain clinical situation (pediatrics, geriatrics, nausea, etc.)
- Suitable for drugs which produce a therapeutic response at very low plasma concentrations.

2.9 Franz's cell apparatus

Franz's cell (Fig. 2.10) are used for *in vitro* study to quantify the release rate of drugs from topical preparation. In these systems, skin membranes or synthetic membranes may be used as barriers to the flow of drug and vehicle to simulate the biological system. The typical of franz's cell has two chambers, one on each side of the test diffusion membrane. A temperature-controlled solution is placed in one chamber and a receptor solution in the others. Drug permeation may be determined by periodic sampling and assay of the drug content in the receptor solution. Franz's cell is the most widely used apparatus to determine the drug release profile from the topical drug products because of the reliability and reproducibility. The test sample is placed in the donor phase, which was separated from the receptor phase by a semipermeable membrane. The suitable receptor medium is suggested to increase the drug solubility for detection of drug release by the ultraviolet spectroscopy or high-pressure liquid chromatography (HPLC) [39].

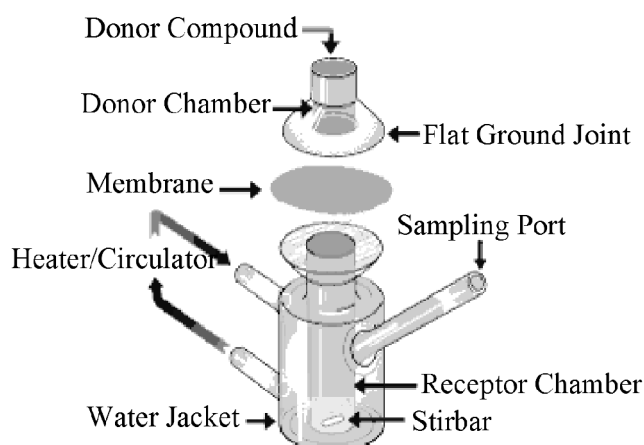


Figure 2.10 The components of Franz's cell [40]

2.10 Skin sources

The difference of skin sources give the different results in percutaneous absorption, these differences are due to the physiology of the skin. The types of skin sources in percutaneous absorption studies were human skin, animal skin and artificial skin and skin cultures.

Human skin

The human skin is the most appropriate choice to predict the percutaneous absorption. In the literatures, the various regions of human skin were used to studies in percutaneous absorption, such as the abdominal skin studies on propranolol [41], bisoprolol [42] and nitrovasodilator drugs [43], the breast skin studies on lorazepam, clonazepam [44] and triclosan [45] and the forearm skin study on capsaicin [46]. The fresh human skin can be obtained from surgery but the availability is limited. Fresh skin can be kept viable for some time allowing some metabolism of the test compound to take place. Since the stratum corneum consist of dead cells, human cadaver skin from autopsies can be used [47].

Animal skin

The animal skin cannot be directly corrected to human skin because animal skin differs from human skin in several ways. Most animals have furry skin and thickness of

the stratum corneum is often thicker than in human skin. The choice of animal skin often depends upon ease of availability and the similar physiological to human skin. The percutaneous absorption has been determined in many animal species, including rats, mice, rabbits, guinea pigs, pigs and snakes. The animal skins that have been used in permeation studies showed in Table 2.1.

Table 2.1 The animal skins that have been used in permeation studies

Species	Permeant	References
Mice	Ketotifen fumarate	Kimura C. et al. 2007 [48]
	Bovine serum albumin	Xie Y. et al. 2005 [49]
	4-nerolidyl-cathecol	Cristina et al. 2002 [50]
Pig	Ketoprofen and propylene glycol	Bowen, Jenna L et al. 2006 [51]
	Moxifloxacin	Kerec M. et al. 2005 [52]
Snake	Ethyl nicotinate	Ngawhirunpat T. et al. 2004 [53]
	lidocaine	Kang L. et al. 2000 [54]

CHAPTER III

MATERIALS AND METHODS

3.1 Materials

The following materials were obtained from commercial suppliers.

3.1.1 Model drugs

Clindamycin hydrochloride (obtained from Siam pharmaceuticals Co., Ltd.)

3.1.2 Polymers and chemicals

- Chitosan with \overline{M}_w of 57 kDa and a degree of deacetylation (DD) of 85% (Seafresh Chitosan (Lab) Company Limited, Thailand)
- Sodium alginate (Carlo Erba Reactifs SA)
- Calcium chloride (Carlo Erba Reactifs SA)
- Acetonitrile, HPLC grade (Merck, Germany)
- Methanol, HPLC grade (Merck, Germany)
- Acetic acid glacial (Carlo Erba Reactifs SA)
- Sodium hydrogen phosphate, AR grade (Merck, Germany)
- Potassium dihydrogen phosphate, AR grade (Merck, Germany)
- Cellulose dialysis membrane with \overline{M}_w cut off at 3,500 Da (Spectrum Laboratories Inc.)
- Cellulose acetate membrane pore size 0.45 μm for Franz diffusion analysis

3.2 Instruments

The instruments used in this study are listed in Table 3.1

Table 3.1 Instruments

Instrument	Manufacture	Model
High voltage	Ormond beach	GAMMA
Syring pump	KDscientific	KD100
Analytical balance	Mettler	AT200
Ultracentrifuge	Refrigerated centrifuge	Sigma 30K
HPLC	ThermoFinnigan	P4000
Particle sizer	Malvern Instruments	Zetasizer nanoseries
Fourier transform infrared spectrometer	Perkin Elmer	Spectrum One
Scanning electron microscope	Philips	XL30CP
Differential scanning calorimeter	NETZSCH	DSC 7
X-ray diffractometer	JEOL	JDX-8030
pH-meter	Metrohm	744
Micropipette (100-10000 μ l)	Mettler Toledo	Volumate
Magnetic stirrer	IKA®C-MAG	HS7
Freez dryer	Labconco	Freeze 6

3.3 Nanospheres preparation

3.3.1 Alginate/chitosan nanospheres preparation

Alginate/chitosan nanospheres were prepared by electrospray technique. A 10 ml of 5 mg/ml alginate solution is ejected from a reservoir using a syringe pump into a syringe-nozzle system. A high electric field applied to the polymer solution in the syringe. Droplets fall into a coagulant bath containing 30 ml of 0.33 mg/ml CaCl_2 solution, stirred at 1000 rpm for 30 min. After that, 10 ml of 0.03 mg/ml chitosan solution was added dropwise into the pre-gel, stirred for an additional 30 min. The nanospheres suspension were kept overnight to stabilization. The nanospheres were separated by ultra centrifugation at 20,000g for 40 min. The preparation of clindamycin-loaded alginate/chitosan nanospheres (CM-ALG/CS-NSs) were prepared following:

Alginate-clindamycin solutions were prepared by adding a specified amount of clindamycin hydrochloride (CM) into the alginate solution under magnetic stirring at 100 rpm for 1 hour. This mixed solution was then used for nanospheres preparation. The parameters studied for the nanospheres preparation by using an electrospray technique are shown in Table 3.2

Table 3.2 The parameters studied for the nanospheres preparation

Applied voltage (kV)	5, 10, 15
Flow rate (mL/h)	10, 15, 20
Needle gauge (g)	18, 20, 26
Working distance	8, 12, 15
Ratio of alginate/chitosan:clindamycin	1:1, 1:2, 2:1

3.4 Characterization of nanospheres

3.4.1 Microscopic analysis

The morphology and surface appearance of particles (before and after the drug loading) were examined by a scanning electron microscope or SEM. The sample was mounted onto an aluminum stub using double-sided carbon adhesive tape and coated with gold-palladium. Coating was achieved at 18 mA for at least 4 min. Scanning was performed under high vacuum and ambient temperature with beam voltage of 10-20 kV.

3.4.2 Particle size measurement

The size measurement of alginate/chitosan nanospheres and CM-ALG/CS-NSs was performed on a particle sizer using He-Ne laser with 4.0 mW power at a 532 nm wavelength. Size calculation was based on DLS method as a software protocol. The scattering light was collected at an angle of 90° through fiber optics and converted to an electrical signal by an avalanche photodiode array (APDs). All samples were sonicated and run in triplicate with the number of runs set to 5 and run duration set to 10 seconds.

In addition, the mean particle size of alginate/chitosan nanospheres was also determined from the scanning electron micrographs, in which the diameters of 100 randomly selected particles were measured by a digital software. The averaged particle size determined by SEM was reported as the size of 'dry' particles.

3.4.3 Zeta potential

Zeta potential of CM-ALG/CS-NSs was determined using particle sizer. The analysis was performed at a scattering angle of 90° . All samples were sonicated and run in triplicate with the number of runs set to 5 and run duration set to 10 seconds.

3.4.4 Functional group analysis

The FT-IR spectra of alginate, chitosan, CM and CM-ALG/CS-NSs were examined by using the potassium bromide disk (KBr) method with a Fourier transform infrared spectrometry (FT-IR) in the range of $4000\text{-}400\text{ cm}^{-1}$.

3.4.5 Powder x-ray diffraction study

CM distribution within the nanosphere was investigated by X-ray diffractometry. The samples for X-ray diffraction studies were firmly packed into a cavity of a thin rectangular metal plate using two glass slides attached to the metal plate with adhesive tape. The first glass slide was then removed, and the prepared sample was taken to expose to the X-ray diffraction chamber. The X-ray diffraction patterns were recorded from 5° to 65° in terms of 2θ angle.

3.4.6 Thermal analysis

Thermal behavior of polyelectrolyte and drug which is correlated in their structure were obtained using Differential Scanning Calorimetry (DSC). Samples were lyophilized, 2.0 mg of lyophilized powder crimped in a standard aluminium pan and heated from 20 to $350\text{ }^\circ\text{C}$ at a heating constant rate of $10\text{ }^\circ\text{C}/\text{min}$ under constant purging of nitrogen at $20\text{ ml}/\text{min}$.

3.5 Determination of drug content and encapsulation efficiency (EE)

The drug content study was done as follows:

The drug content of CM-ALG/CS-NSs was quantitatively determined by immersing the dried nanospheres (10 mg) in 100 ml of distilled water to dissolve the drug dispersed inside the nanospheres. After stirring at 500 rpm for 24 h, the suspension was collected and the total drug content entrapped inside the nanospheres was determined by HPLC. All experiments were performed in triplicates. The CM content was calculated from the following equation:

$$\text{Amount of CM (mg/mg of CM - ALG/CS- NSs)} = \frac{\text{Concentration of clindamycin (mg/mL)}}{10 \text{ mg}} \times 100 \text{ mL}$$

The concentration of clindamycin, CM was calculated from the calibration curve of CM in distilled water.

3.5.1 Calibration curve of clindamycin in distilled water

In order to make a standard curve, 10 mg of CM was accurately weighed into a 100 mL volumetric flask. The distilled water was added to dissolve the CM. The solution was adjusted to volume, and used as stock solution. The stock solution was individually pipetted (0.25, 1.25, 2.5, 5, and 12.5 mL) into a 25 mL volumetric flask by micropipette and adjusted the volume with distilled water. The final concentrations of each solution were 1, 5, 10, 20 and 50 mg/L, respectively.

The known of CM concentration was determined by HPLC. The column used was a reversed phase C18 column (pinnacle, 250 × 4.6 mm). The mobile phase were phosphate buffer pH 7.4 and acetonitrile (55:45 v/v). The flow rate was 1 mL/min and the effluent was monitored at 210 nm. The peak area and the calibration curves of

clindamycin in phosphate distilled water are presented in Table 1B and Figure 1B, respectively, in Appendix B.

The drug encapsulation efficiency study was done as follows:

To determine of the drug encapsulation efficiency of CM-ALG/CS-NSs was quantitatively determined by ultracentrifugation of samples. About 10 mg of sample was suspended in 100 mL phosphate buffer pH 7.4 and after centrifuge, the amount of free drug in clear supernatant was determined by HPLC. All experiments were performed in triplicates. The drug encapsulation efficiency was calculated from the following equation:

$$\% \text{ EE} = \frac{\text{Clindamycin content in ALG/CS - NSs from experimental}}{\text{Clindamycin content in ALG/CS - NSs from theory}} \times 100 \text{ mL}$$

The concentration of clindamycin was calculated from the calibration curve of CM in phosphate buffer saline pH 7.4.

3.5.2 Calibration curve of clindamycin in buffer solution

In order to make a standard curve, 10 mg of CM was accurately weighed into a 100 mL volumetric flask. The phosphate buffer was added to dissolve the CM. The solution was adjusted to volume, and used as stock solution. The stock solution was individually pipetted (0.25, 1.25, 2.5, 5, and 12.5 mL) into a 25 mL volumetric flask using micropipette and adjusted the volume with phosphate buffer pH 7.4. The final concentrations of each solution were 1, 5, 10, 20 and 50 mg/L, respectively.

The known of CM concentration was determined by HPLC. The column used was a reversed phase C18 column (pinnacle, 250 × 4.6 mm). The mobile phase were phosphate buffer pH 7.4 and acetonitrile (55:45 v/v). The flow rate was 1 mL/min and the effluent was monitored at 210 nm. The peak area and the calibration curves of

clindamycin in phosphate buffer pH 7.4 are presented in Table 2B and Figure 2B, respectively, in Appendix B.

3.6 *In vitro* clindamycin release from clindamycin- loaded alginate/chitosan nanospheres

3.6.1 Preparation of buffer medium for drug release study

The phosphate buffer with pH of 7.4 was used as medium for drug release study. The buffer was composed of 0.2 M sodium phosphate dibasic (454.25 mL) and 0.1 M citric acid (45.75 mL).

3.6.2 *In vitro* drug release

The release of CM from nanospheres was performed using the dialysis bag diffusion technique [10]. A 10 mg of CM-ALG/CS-NSs were suspended in 3 mL phosphate buffer pH 7.4 and placed in the dialysis bag with a molecular weight cutoff of 3500 Da, hermetically sealed and immersed in 100 mL of phosphate buffer pH 7.4 at $37\pm 1^\circ\text{C}$ under stirred condition at 200 rpm. Samples of 5 mL was withdrawn at the time intervals of 1, 2, 4, 6, 8, 10 and 12 h. An equal volume of the fresh buffer was replaced immediately after each sampling in order to keep a constant volume of the buffer in the vessel throughout the experiment.

Each sampling solution was filtered through nylon filters (0.45 μm , Whatman, England) and assayed for the drug released by measuring the peak area by HPLC. The amount of CM at time intervals was calculated from the calibration curve for each buffer medium. Each experiment was performed in triplicate. The amount of cumulative CM release are presented in Table 1C, 2C and 3C, respectively, in

Appendix C. The percentage of cumulative CM release are presented in Table 1D, 2D and 3D, respectively, in Appendix D.

The amount of CM released was calculated by interpolation from a calibration curves containing increasing concentrations of CM and the percentage of cumulative CM release was calculated from the following equations:

$$\begin{aligned} & \text{Amount of CM release (mg/mg of CM - ALG/CS- NSs)} \\ & = \frac{\text{Concentration of clindamycin (mg/mL)}}{10 \text{ mg}} \times 100 \text{ mL} \end{aligned}$$

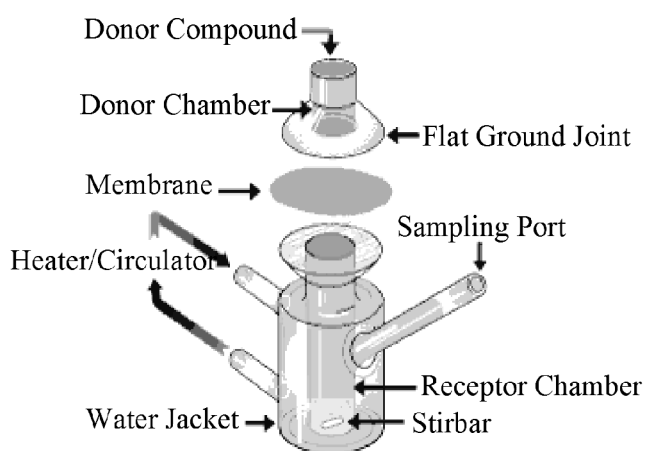
% Cumulative release

$$= \frac{\text{Amount of clindamycin from releasing (mg/mg of CM - ALG/CS- NSs)}}{\text{Amount of clindamycin before releasing (mg/mg of CM - ALG/CS- NSs)}} \times 100 \text{ mL}$$

3.7 *In vitro* study of drug permeation through cellulose membrane

3.7.1 Drug permeation studies

The release of CM permeation study was performed using Franz diffusion cell. Cellulose membrane with pore size of 0.45 μm was fitted into place between the donor and receptor chambers. The upper donor chamber was filled with 10 mg of CM-ALG/CS-NSs in phosphate buffer pH 7.4. The diameter of the Franz's cell was 1.5 cm corresponding to an effectively permeable area of 1.77 cm^2 . The receptor chambers contained 12 mL of phosphate buffer pH 7.4 as the receptor fluid. The receptor phase was stirred at 500 rpm during the study and the temperature was maintained at 37°C by circulating water through a jacket surrounding the cell body throughout the experiment. One milliliter of receptor fluid was withdrawn at 1, 2, 4, 6, 8, 10 and 12 h. Fresh buffer was replaced after each collection. The release of CM were analyzed using HPLC according to the method outlined above. Each test was carried out in triplicate and the mean of three observations was reported



(a)



(b)

Figure 3.1 The components of Franz's cell and instrument set-up for permeation study

The cumulative amount of drug permeated through a unit area of the membrane was calculated from the following equations:

$$Q_p = \frac{C_{CM} \times V_B}{A_M}$$

where Q_p is the cumulative amount of drug permeated through a unit area of cellulose membrane ($\mu\text{g}/\text{cm}^2$), C_{CM} is the concentration of CM permeated in receptor (mg/mL), V_B is the volume of buffer pH 7.4 (12 mL for this experiment) in the receptor, A_M is the area of cellulose membrane (1.77 cm^2 for this experiment).

The cumulative amount of drug permeated through a unit area of cellulose membrane are presented in Table 1E-4E, in Appendix E

The flux of CM from CM-ALG/CS-NSs in the receptor compartment obtained from the slope of the linear correlation between cumulative amount of drug (Q_p) and time are presented in Figure 1E-4E, in Appendix E.

3.7.2 Buffer medium preparation

Preparation of phosphate buffer pH 7.4 was the same as the method used in the *in vitro* release study. The buffer was composed of 0.2 M sodium phosphate dibasic (454.25 mL) and 0.1 M citric acid (45.75 mL).

3.7.3 Pretreatment of cellulose membrane

Prior to the experiment, the cellulose membranes were cut into pieces of $2 \times 2 \text{ cm}^2$ each in size. They were then soaked in buffer medium (pH 7.4) for 12 hours before used.

3.8 Antibacterial Activity of drug loaded ALG/CS-NSs

Antibacterial activity was studied on an clindamycin sensitive bacterial strain *S. aureus*. Bacterial cells were revived in nutrient broth and 100 μL of the liquid media was spread-plated onto nutrient agar plates. Following this, wells were generated in the center of the plates using a borer. In the first set of plates, 2.5 mg of CM-ALG/CS-NSs dispersed in PBS (pH 7.4, 0.2M) were placed in the wells. In the second set, clindamycin alone was placed in wells and, in the third set unloaded ALG/CS-NSs dispersed in PBS were placed in the wells. The plates of all the three sets were then incubated overnight at 37°C and observed for zone of inhibition.

3.9 Statistical analysis

All measurements were performed in triplicate for each experiment. Results are presented as means \pm SD. Statistical analysis was performed by one-way ANOVA using Microsoft Excel (Microsoft Corporation) with $P < 0.05$ considered to indicate statistical significance.

CHAPTER IV

RESULTS AND DISCUSSION

4.1 Synthesis and optimization of fabrication parameter

The ALG/CS-NSs were formed using electrospray technique. The spherical sizes were determined by size measurement from scanning electron micrographs (SEM) and by a particle sizer. The SEM technique was used to measure the size of dry particles, while the particle sizer was performed on hydrated samples. It is noteworthy that the particle sizes measured by the particle sizer are mostly higher than the size estimated from the SEM particularly because of the high swelling capacity of ALG/CS-NSs. Effect of the process parameters such as voltage, flow rate, needle gauge and working distance were studied and the results obtained were as follows:

The size of ALG/CS-NSs obtained from SEM and particle sizer upon varying the voltage applied on polymer are presented in Table 4.1

Table 4.1 Effect of voltage on spherical size of ALG/CS

Voltage (kV)	Particle size ^a (nm ± SD)	Particle size ^b (nm ± SD)	PDI ^c
5	921 ± 132	1219 ± 371	0.844
10	490 ± 120	881 ± 324	0.811
15	212 ± 25	855 ± 92	0.854
	$p = 4.662 \times 10^{-15}$	$p = 0.023079$	

^aParticle size measured by SEM, ^b Particles size measured by particle sizer

^cPolydispersity index from particle sizer

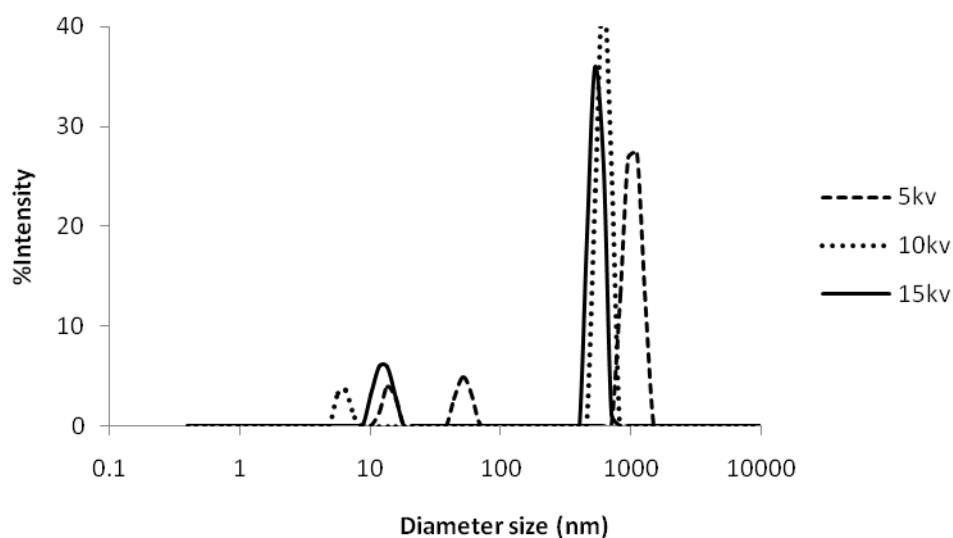


Figure 4.1 Effect of voltage on size and size distribution measured by particle sizer

The effect of voltage on nanosphere formation was studied by varying the applied voltage values from 5 to 15 kV. While, the flow rate of the alginate solution through the needle tip and the working distance were kept constant at 10 mL/h, 26g and 8 cm, respectively. The applied voltage effect on the breakdown of the jet, so when increasing voltages, the jet current was increased and led to smaller sphere sizes. SEM analysis revealed that when the voltage increased from 5-15 kV, the sphere size decreased from 921 ± 132 to 212 ± 25 nm while the sphere size obtained from the particle sizer decreased from 1219 ± 371 to 855 ± 92 nm. The observed change in sphere size can be attributed to the Rayleigh limit, that is the magnitude of charge on a drop that overcome the surface tension force, leads to a fission of the droplet [19]. Therefore, at lower voltage, there is a few of charge on a drop, so large spheres with irregular shape are formed. Whereas at higher voltage, there is a lot of charge on a drop, so the jet deforms and disrupts into droplets due to electrical force resulting to a smaller sphere size. Moreover, the size distribution of all voltage is narrow (Fig. 4.1).

The size of ALG/CS-NSs obtained from SEM and particle sizer upon varying the flow rate of alginate solution are presented in Table 4.2.

Table 4.2 Effect of flow rate on spherical sizes of ALG/CS

Flow rate (mL/h)	Particle size ^a (nm ± SD)	Particle size ^b (nm ± SD)	PDI ^c
10	212 ± 25	855 ± 92	0.920
15	450 ± 120	959 ± 226	0.870
20	521 ± 143	965 ± 161	0.850
	$p = 7.534 \times 10^{-6}$	$p = 0.318678$	

^aParticle size measured by SEM, ^b Particles size measured by particle sizer

^cPolydispersity index from particle sizer

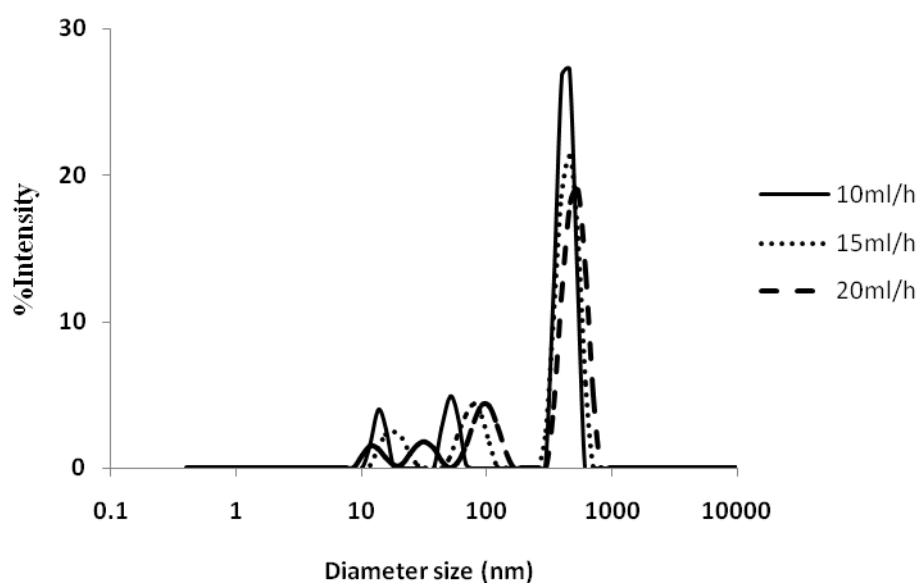


Figure 4.2 Effect of flow rate on size and size distribution measured by particle sizer

To study the effect of the alginate solution pump flow rate on the nanospheres size, the applied voltage, needle gauge and working distance were kept constant at 15 kV, 26g and 8 cm, respectively. When changing flow rate from 10-20 mL/h, the sphere obtained increased in size proportional to the increment of flow rate, the sphere size obtained from SEM were from 212 ± 25 to 521 ± 143 nm while the sphere size obtained from the particle sizer were from 855 ± 92 to 965 ± 161 nm. This can be simply explained by the fact that the solution flowing out from a needle which caused elongation of the meniscus to a form of jet. Therefore, at low flow rate, the droplets are formed at a rate, which is optimum to spraying of the polymer solution with the formation of stable jet, which results in the formation of smaller sphere size. Whereas, at high flow rate, the effective flow rate of polymer solution increases and the drops are formed very quickly led to formed of larger sphere size. At low flow rate 10 mL/h, the size distribution is narrow (Fig. 4.2).

The effect of needle gauge on sphere size was studied as presented in Table 4.3. The voltage, flow rate and working distance were kept at 15 kV, 10 mL/h and 8 cm, respectively.

Table 4.3 Effect of needle gauge on spherical size of ALG/CS

Needle gauge (g)	Particle size ^a (nm \pm SD)	Particle size ^b (nm \pm SD)	PDI ^b
18	882 ± 135	1035 ± 213	0.885
20	342 ± 54	874 ± 314	0.885
26	212 ± 25	855 ± 92	0.920
	$p = 2.682 \times 10^{-16}$	$p = 0.201248$	

^aParticle size measured by SEM, ^b Particles size measured by particle sizer

^cPolydispersity index from particle sizer

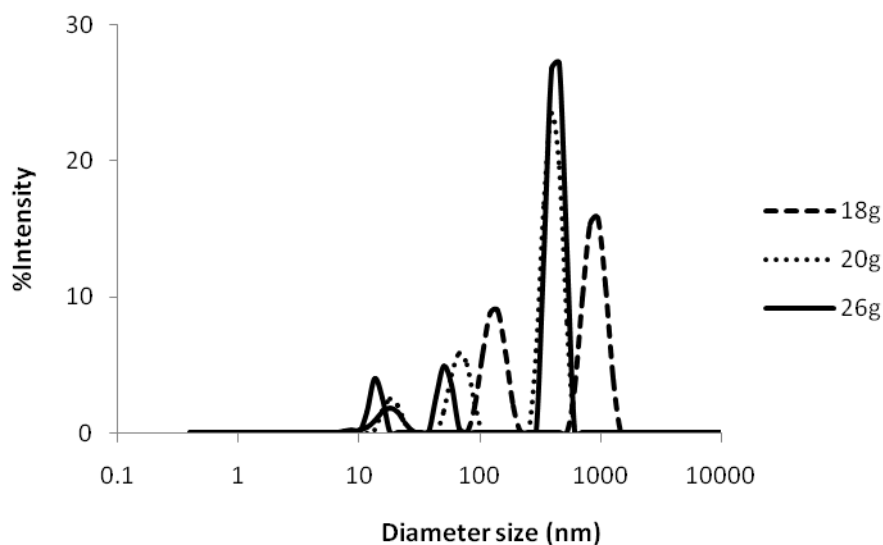


Figure 4.3 Effect of needle gauge on size and size distribution measured by particle sizer

The diameter of a needle is inversely proportional to its gauge and hence smaller needles have a higher value of gauge. The needle gauges used were 18, 20 and 26g (with internal diameter (I.D.) of 0.838, 0.584 and 0.241 mm respectively). When increasing the needle gauge, the sphere size was decreased. The sphere size obtained from 18-26g were 882 ± 135 to 212 ± 25 nm measured from SEM and the sphere size reported from particle sizer analysis were 1035 ± 213 to 855 ± 92 nm. The observed changes in the sphere size can be illustrated that in case of 18 and 20g, a lot of polymer solution flow out from the needle tip when applied voltage be equal to 26g, the surface charge on drop less than in case of 26g which in effect led to larger sphere size. In the case of size distribution (Fig. 4.3), 26g is narrower in size distribution more than 18g and 20g.

The influence of working distance on the size of sphere formed was studied as presented in Table 4.4.

Table 4.4 Effect of working distance on spherical size of ALG/CS

Working distance (cm)	Particle size ^a (nm ± SD)	Particle size ^b (nm ± SD)	PDI ^b
8	212 ± 25	855 ± 92	0.920
12	303 ± 51	979 ± 249	0.868
15	343 ± 43	1144 ± 519	0.910
	$p = 5.125 \times 10^{-6}$	$p = 0.210793$	

^aParticle size measured by SEM, ^b Particles size measured by particle sizer

^cPolydispersity index from particle sizer

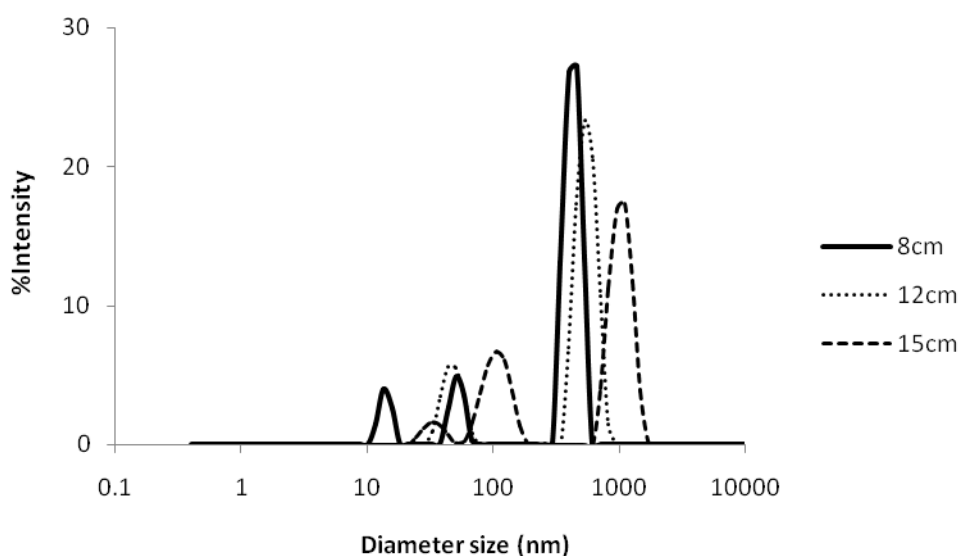


Figure 4.4 Effect of working distance on size and size distribution measured by particle sizer

The parameter range studied was from 8 to 12 cm while other parameters such as voltage, flow rate and needle gauge were kept constant at 15 kV, 10 mL/h and 26g, respectively. It can be clearly seen that the sphere size was increasing with increased

working distance, the sphere size obtained from SEM increased from 212 ± 25 to 343 ± 43 nm and the sphere size obtained from the particle sizer increased from 855 ± 92 to 1144 ± 519 nm. It suggest that at working distance of 8 cm, the sphere size was found to be smaller than another working distance due to increase in the electric field strength, which in effect raise the rate of sphere formation led to smaller sphere size. Whereas at the large of working distance 12 cm, the electric field strength decreased, which in effect might have reduced the rate of sphere formation and led to larger sphere size. At 8 cm of working distance is narrow size distribution (Fig. 4.4)

Drug loaded ALG/CS-NSs were prepared by using the result from the optimization studied. Alginate to clindamycin mass ratios of 1:0.5, 1:1 and 1:2 were employed for all the experiment and presented in Table 4.5. All the other fabrication parameters were kept constant at the optimized value obtained from the previous set of experiment, and the value used were, voltage of 15 kV, flow rate of 10 mL/h, needle gauge of 26g and working distance of 8 cm.

Table 4.5 Effect of mass ratio of alginate to clindamycin on spherical size of ALG/CS and zeta potential produced by optimal condition (ALG:CM=1:0)

Mass ratio ALG:CM	Particle size ^a (nm \pm SD)	Particle size ^b (nm \pm SD)	PDI ^b	Zeta potential (mV \pm SD)
1:0	212 ± 25	855 ± 92	0.920	-45.10 ± 2.26
1:0.5	518 ± 55	1000 ± 367	0.936	-54.12 ± 4.21
1:1	522 ± 46	1013 ± 280	0.950	-46.07 ± 2.82
1:2	550 ± 80	1018 ± 226	0.901	-49.63 ± 2.34
	$p = 7.38 \times 10^{-6}$	$p = 0.991076$		

^aParticle size measured by SEM, ^b Particles size measured by particle sizer

^cPolydispersity index from particle sizer

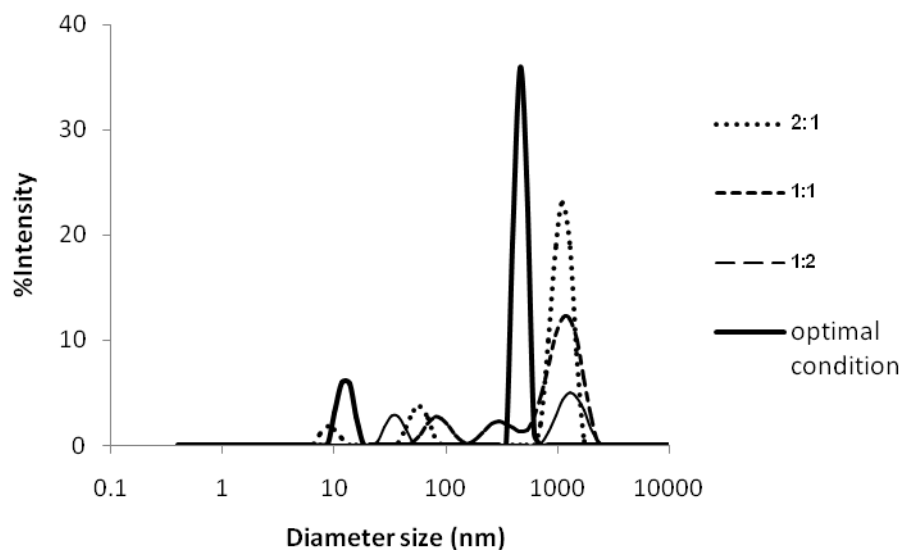


Figure 4.5 Effect of ALG:CM mass ratio on size and size distribution measured by particle sizer

The effect of alginate to clindamycin mass ratio on sphere size and zeta potential was studied as presented in Table 4.5. The size of ALG/CS increased with the increasing drug content were obtained from SEM analysis and the particle sizer. The results indicated that the drug content did not significantly affect the size of CM-ALG/CS-NSs when the drug content was ranged from 1:0.5 to 1:2. When considering the zeta potential, that is surface charge, it can greatly influence particle stability in suspension through the electrostatic repulsion between particles [20]. The surface of ALG/CS-NSs was found to possess negative charge of -45.10 mV and the surface charge of CM-ALG/CS-NSs with mass ratios of 1:0.5, 1:1, and 1:2 were found to be negative -54.12, -46.07, and -49.63 mV respectively. This result explained that the amount of alginate, which is negative charge more than chitosan cause the surface charge on droplet was negative.

In case of size distribution of various ALG:CS mass ratios (Fig 4.5), the unload ALG/CS-NSs has a narrower size distribution than the loaded ALG/CS-NSs. In addition, when ALG:CM mass ratios increased it results in widely size distribution.

4.2 Characterization of nanospheres

4.2.1 Morphology

The SEM micrographs of nanospheres were shown in Figure 4.6. The surface morphological appearance of ALG/CS-NSs was compared with the CM-ALG/CS-NSs. Without clindamycin (Fig 4.6a-b), the ALG/CS-NS was in a generic spherical shape. Smoothness on the surface could be clearly seen at high magnification. In case of clindamycin-containing spheres, the surface of some CM-ALG/CS-NS (Figs. 4.6c) exhibited rough feature that was possibly related to the incorporated clindamycin on the sphere surface and cracking at the surface area cause from electron bombardment.

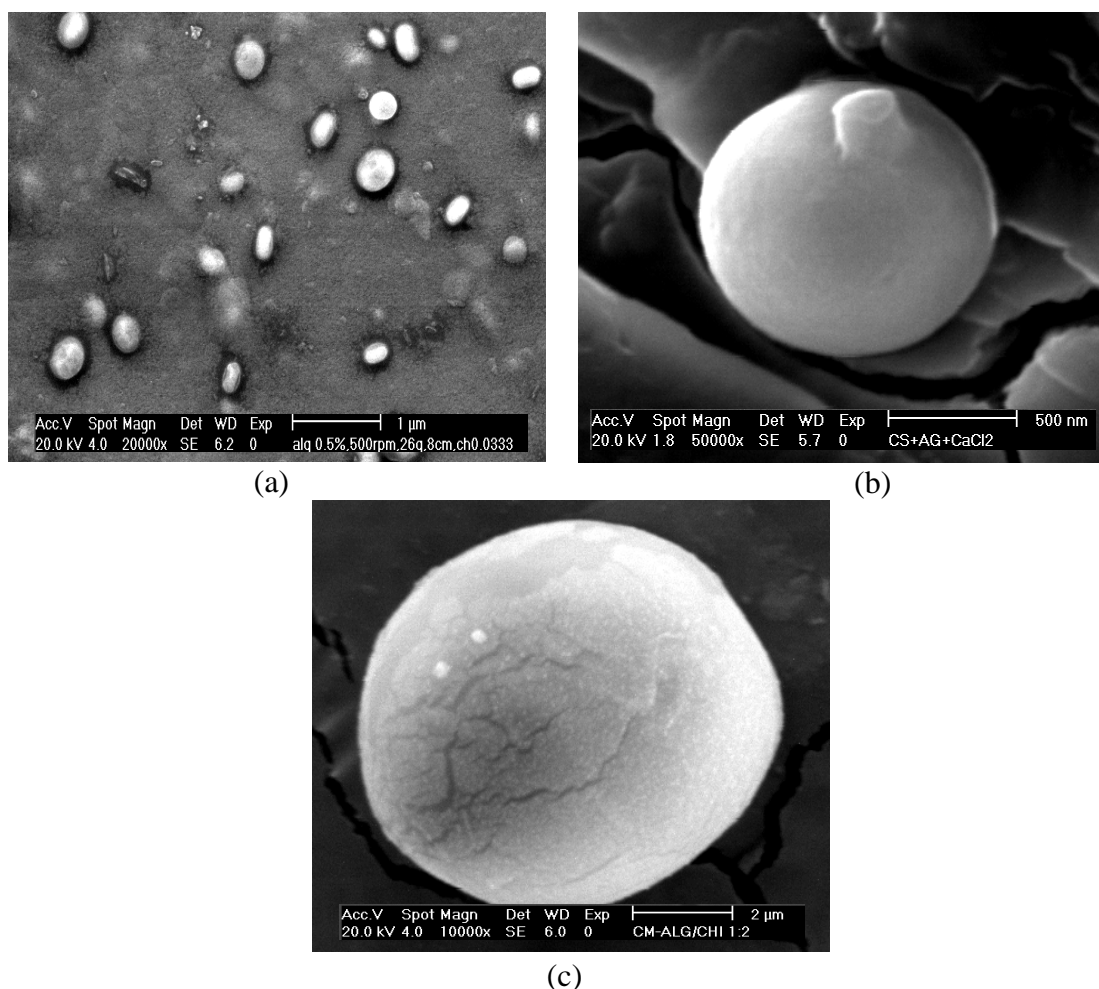


Figure 4.6 Scanning electron micrograph of ALG/CS-NSs without CM (a) at 20000x and (b) at 50000x. ALG/CS-NSs with CM (c) at 10000x (applied voltage 15 kV, flow rate 10 ml/h, needle gauge 26g and working distance 8 cm)

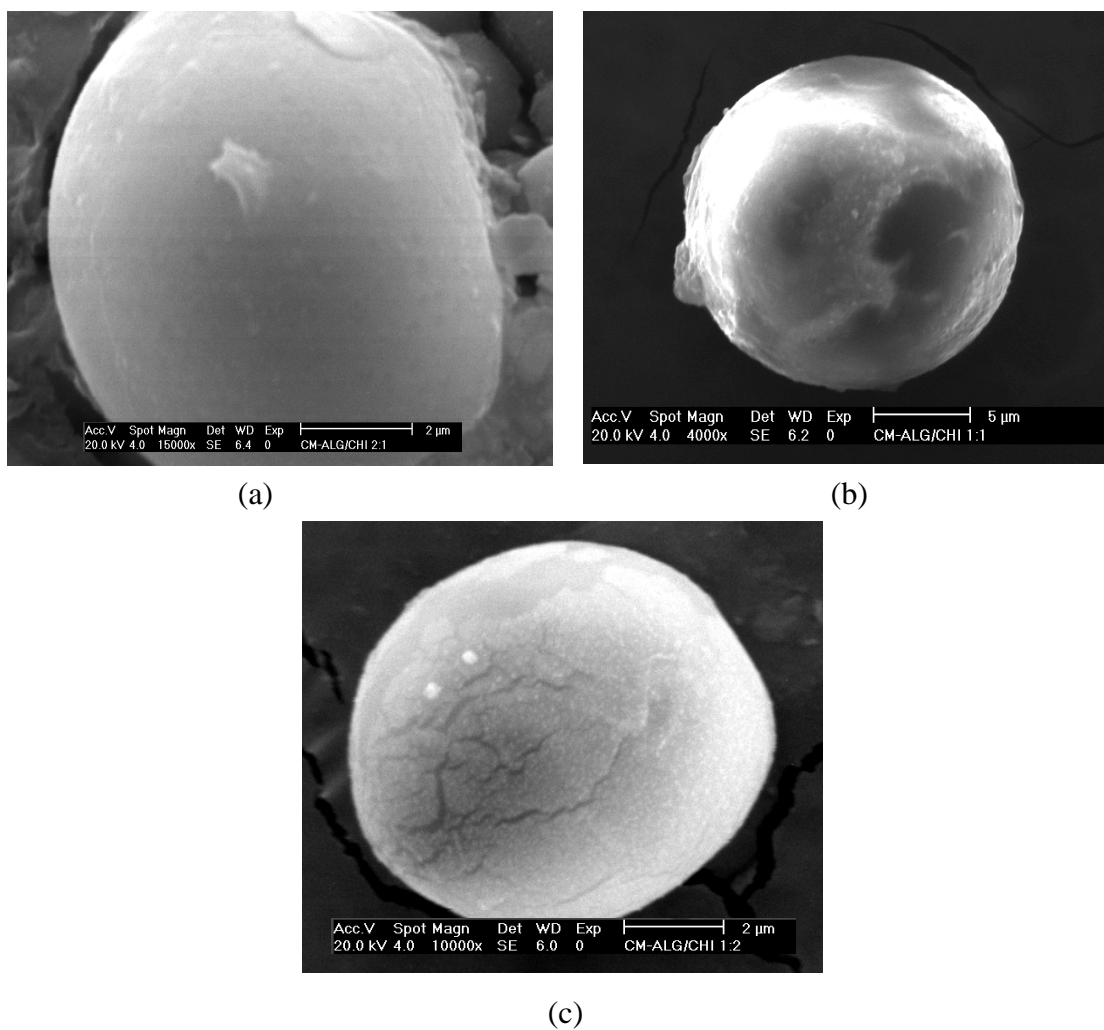


Figure 4.7 Scanning electron micrographs of CM-ALG/CS-NSs at ALG:CM ratio of (a) 1:0.5, (b) 1:1, and (c) 1:2 (applied voltage 15 kV, flow rate 10 mL/h, needle gauge 26g and working distance 8 cm)

In case of clindamycin-containing spheres with different alginate to CM mass ratios (Fig. 4.7), the surface of all mass ratios exhibited the incorporated of clindamycin on the spheres surface. It was corresponding to mass ratio of polymer to drug given and the encapsulation efficiency of CM-ALG/CS-NSs which affected the drug content on spheres surface.

4.2.2 Fourier transform infrared spectroscopy (FTIR)

FTIR spectroscopy was used to determine the chemical interaction of the samples as displayed in Figures 4.8

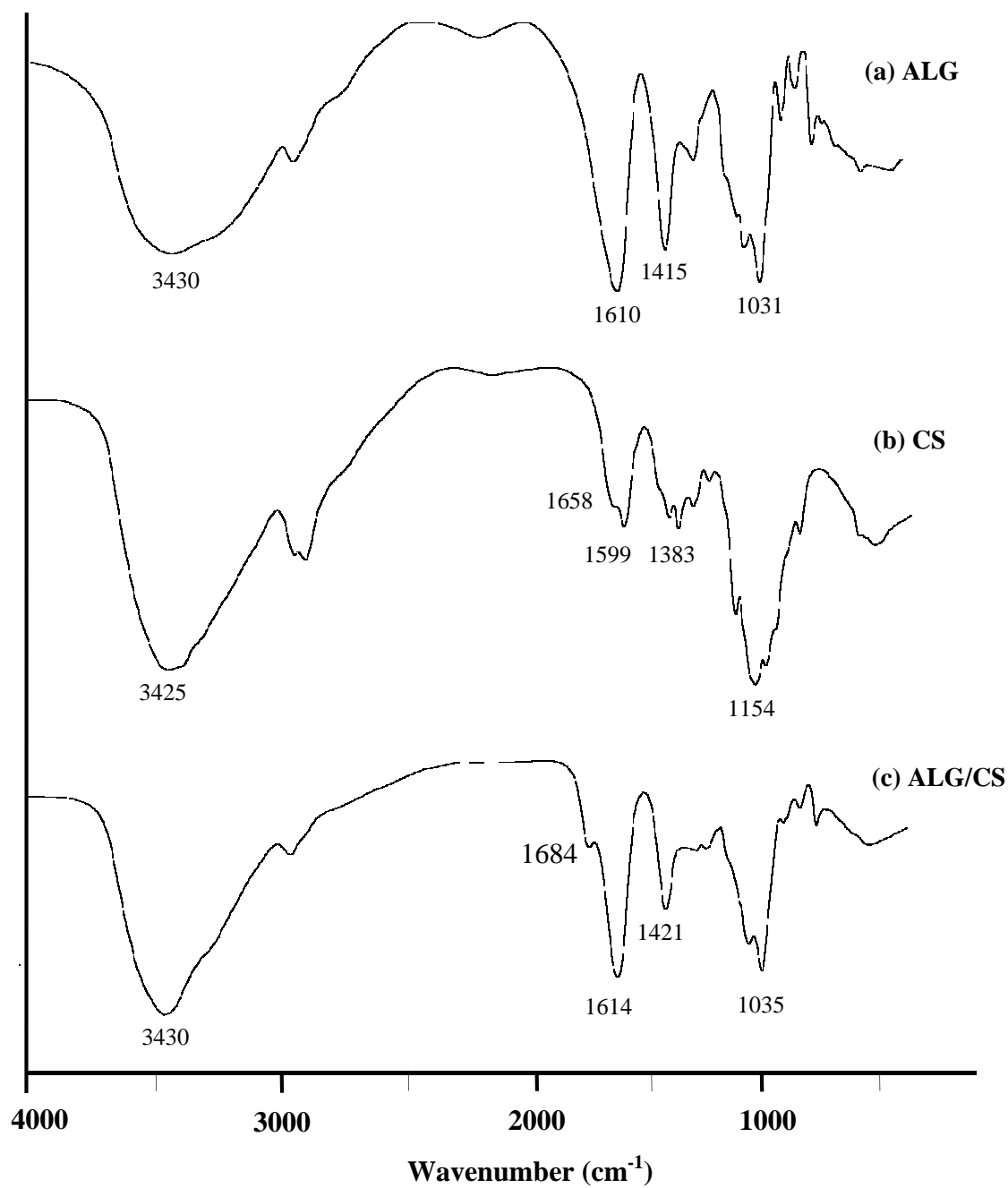


Figure 4.8 FTIR spectra of (a) alginate, (b) chitosan, and (c) ALG/CS-NSs

Fig. 4.8 represents IR spectra of pure alginate, chitosan and ALG/CS-NSs. The IR spectrum of alginate (Fig. 4.8a) showed a distinct peak at 3430 cm^{-1} which was due to the O-H groups presented on the structure. The symmetric peak around 1610 cm^{-1} and the asymmetric peak around 1415 cm^{-1} was due to COO^- stretching vibration. The peak at 1031 cm^{-1} was due to C-O-C stretching in the intra- and intermolecular between polymer's repeating units.

The IR spectrum of chitosan (Fig. 4.8b) also showed the peak at 3425 cm^{-1} corresponding to the O-H stretching. The small peak of amide bond at 1658 cm^{-1} and a small protonated amino peak at 1599 cm^{-1} resulting from partial *N*-deacetylation of chitin. The peak near 1383 cm^{-1} which was due to $-\text{CH}_3$ bending and the peak at 1154 cm^{-1} was attributed to C-O-C stretching.

The IR spectrum of ALG/CS-NSs (Fig. 4.8c) showed the peak at 3430 cm^{-1} corresponding to O-H stretching. The small peak at 1684 cm^{-1} was due to C=O stretching of amide bond and shifted from 1658 cm^{-1} after complexation with chitosan and absent in alginate. The distinct peak at around 1614 cm^{-1} was due to the symmetric COO^- stretching vibration and also shifted from 1610 cm^{-1} after complexation with alginate. The peak near 1421 cm^{-1} was due to the asymmetric COO^- stretching vibration of carboxyl group in alginate and the peak at around 1035 cm^{-1} was attributed to C-O-C stretching.

It could imply that the observed changes in the absorption bands of the amino, carboxyl and amide groups can be attributed to an ionic interaction between the carboxyl group of alginate and the amino group of chitosan [55].

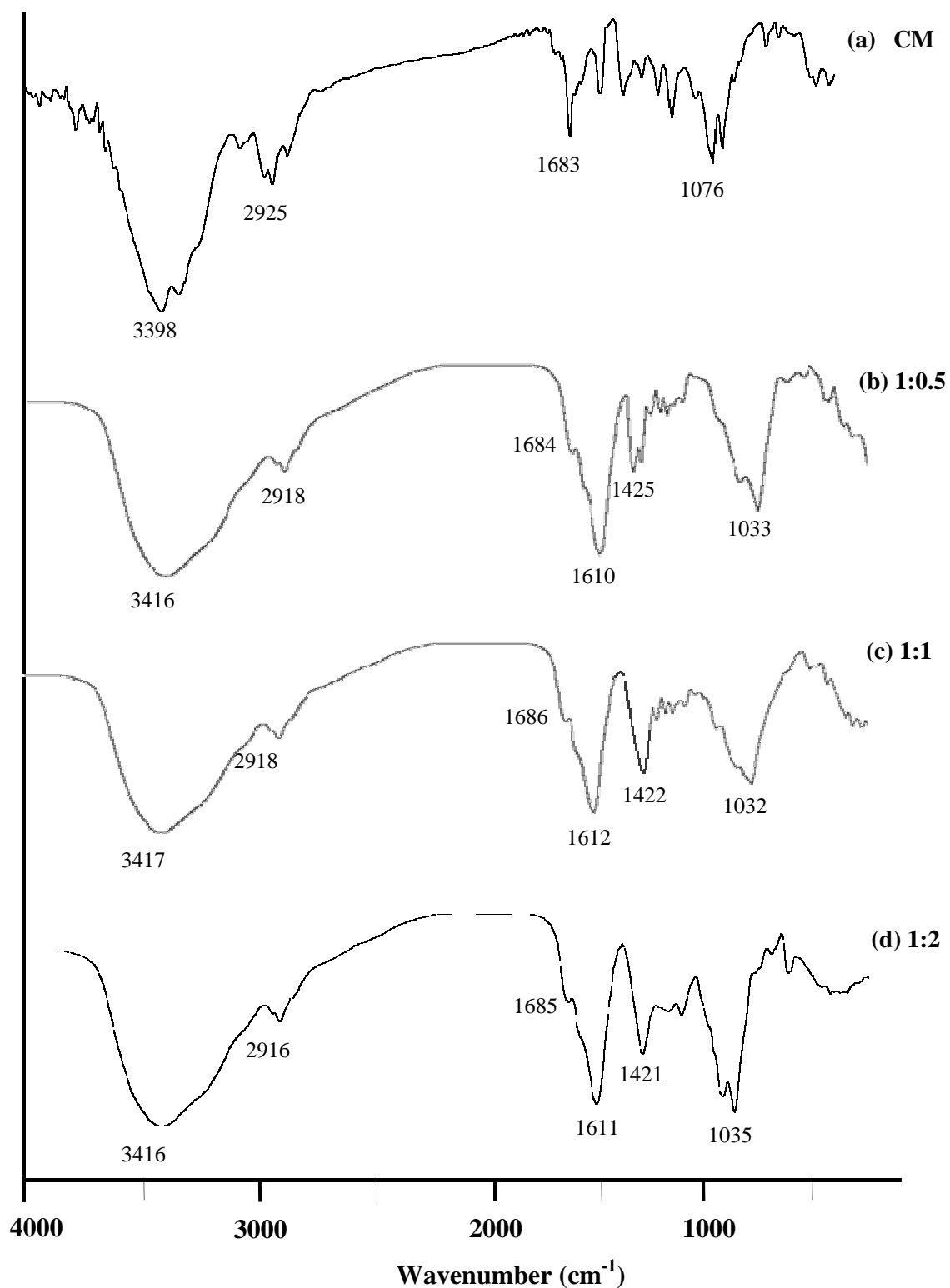


Figure 4.9 FTIR spectra of (a) clindamycin, (b) CM-ALG/CS-NSs (ALG:CM = 1:0.5), (c) CM-ALG/CS-NSs (ALG:CM = 1:1) and (d) CM-ALG/CS-NSs (ALG:CM = 1:2)

The introduction of CM into ALG/CS-NSs was also investigated by FTIR analysis of CM-ALG/CS-NSs. The obtained spectra are presented in Fig. 4.5.

The IR spectrum of CM (Fig. 4.9a) showed the distinct peak at around 3398 cm^{-1} that was assigned to O-H stretching vibration, and the band at around 2925 cm^{-1} was assigned to -CH stretching vibration. The characteristic peak near 1683 cm^{-1} corresponding to C=O stretching of amide bond. The peak at around 1076 cm^{-1} was attributed to C-O-C stretching.

The IR spectra of CM-ALG/CS-NSs with different alginate to CM mass ratio, ALG:CM = 1:0.5, 1:1 and 1:2 were showed in fig. 4.9 (b), (c), and (d), respectively. In Fig. 4.5b, the band centered at around 3416 cm^{-1} was assigned to O-H stretching vibration and the band at around 2918 cm^{-1} was assigned to -CH stretching vibration. The shoulder peak at around 1683 cm^{-1} was due to C=O stretching of amide bond. The distinct peak at 1610 cm^{-1} and 1425 cm^{-1} were due to symmetric COO^- and asymmetric stretching vibration respectively. The peak around 1033 cm^{-1} assigned to C-O-C stretching. The characteristic peak of CM around 1683 cm^{-1} , concerned to the stretching vibration of C=O stretching shifted to the wave number around 1684 cm^{-1} . When considering another mass ratio of alginate to CM, their IR spectra have the similarly peak positions of CM but might be shifted by a few wavenumber from pure CM.

Therefore, the results showed that there was the non-covalent intramolecular interactions between O-H group of CM and amino group of chitosan and the new absorption bands of drug-loaded nanospheres were not presented. It was possible there was not changed in structure of CM within ALG/CS-NSs.

4.2.3 Powder x-ray diffraction (XRD)

The X-ray powder diffraction patterns of alginate, chitosan, ALG/CS-NSs, clindamycin and CM-ALG/CS-NSs showed in Figure 4.6.

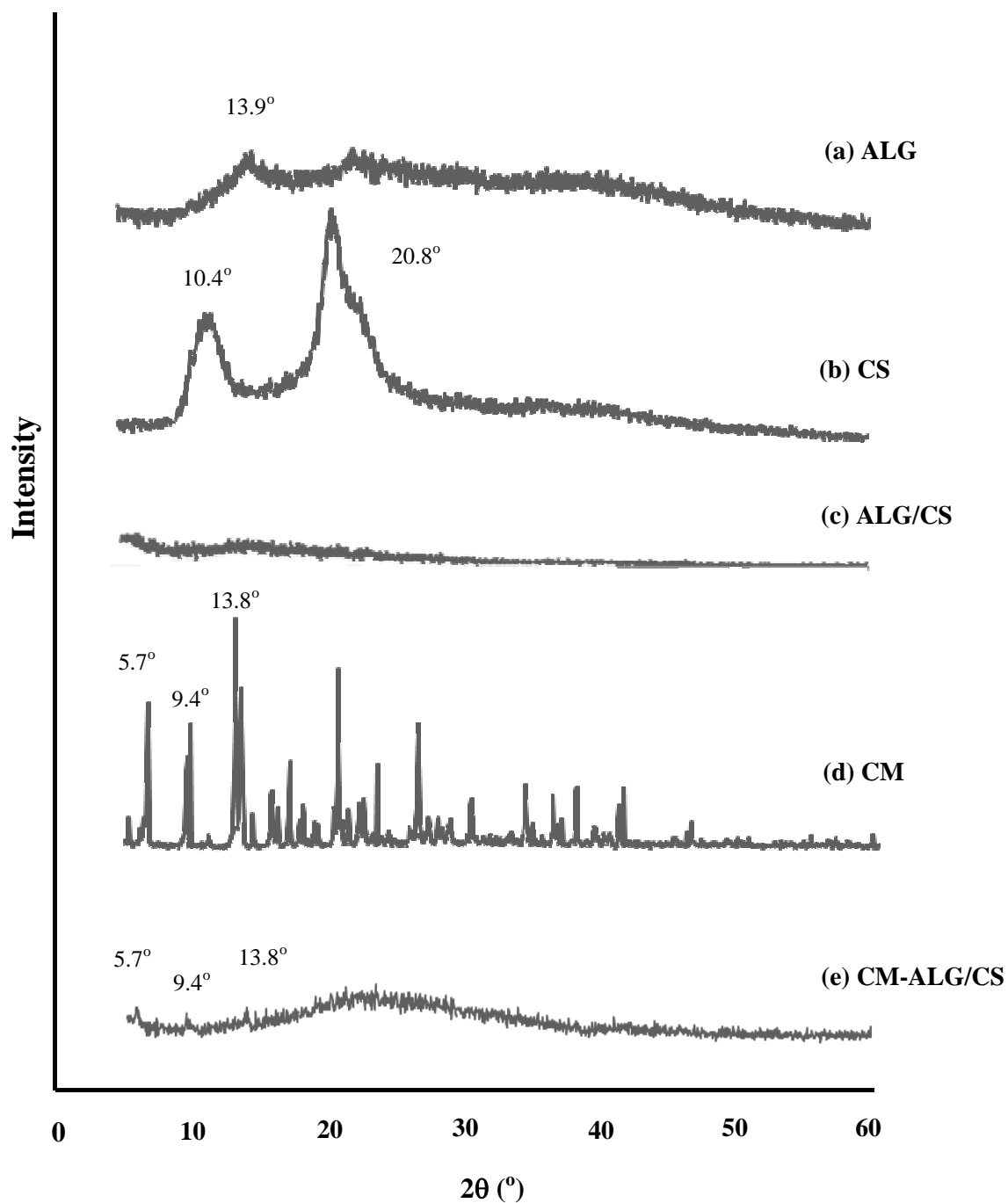


Figure 4.10 X-ray diffractograms of (a) alginate, (b) chitosan, (c) ALG/CS-NSs (d) Clindamycin and (e) CM-ALG/CS-NSs

The diffractogram of alginate (Fig. 4.10a) exhibits a very small crystallinity and showed broad peak at $2\theta = 13.9^\circ$ [56]. The diffractogram of chitosan (Fig. 4.6b) showed two strong crystalline peaks at $2\theta = 10.4^\circ$ and 21.8° [57]. When chitosan was mixed into the alginate (Fig. 4.10c), the crystalline peak disappeared. It could imply that the crystallinity of CS was disrupted after being combined with alginate via electrostatic interactions. The diffractogram of CM (Fig. 4.10d) showed the characteristic peaks at 2θ of 5.7° , 9.4° and 13.8° . The diffractogram of CM-ALG/CS-NSs (Fig. 4.10e) showed the low intensity crystalline peaks at the same positions of the characteristic peaks of CM. This could be explained that CM dispersed into ALG/CS chains and it was entrapped within ALG/CS-NSs.

4.2.4 Differential scanning calorimetry (DSC)

Differential scanning calorimetry was used to characterize the thermal behavior of polyelectrolytes and drug which was correlated to their structure. The DSC thermograms of nanospheres are shown in Figure 4.11 and 4.12

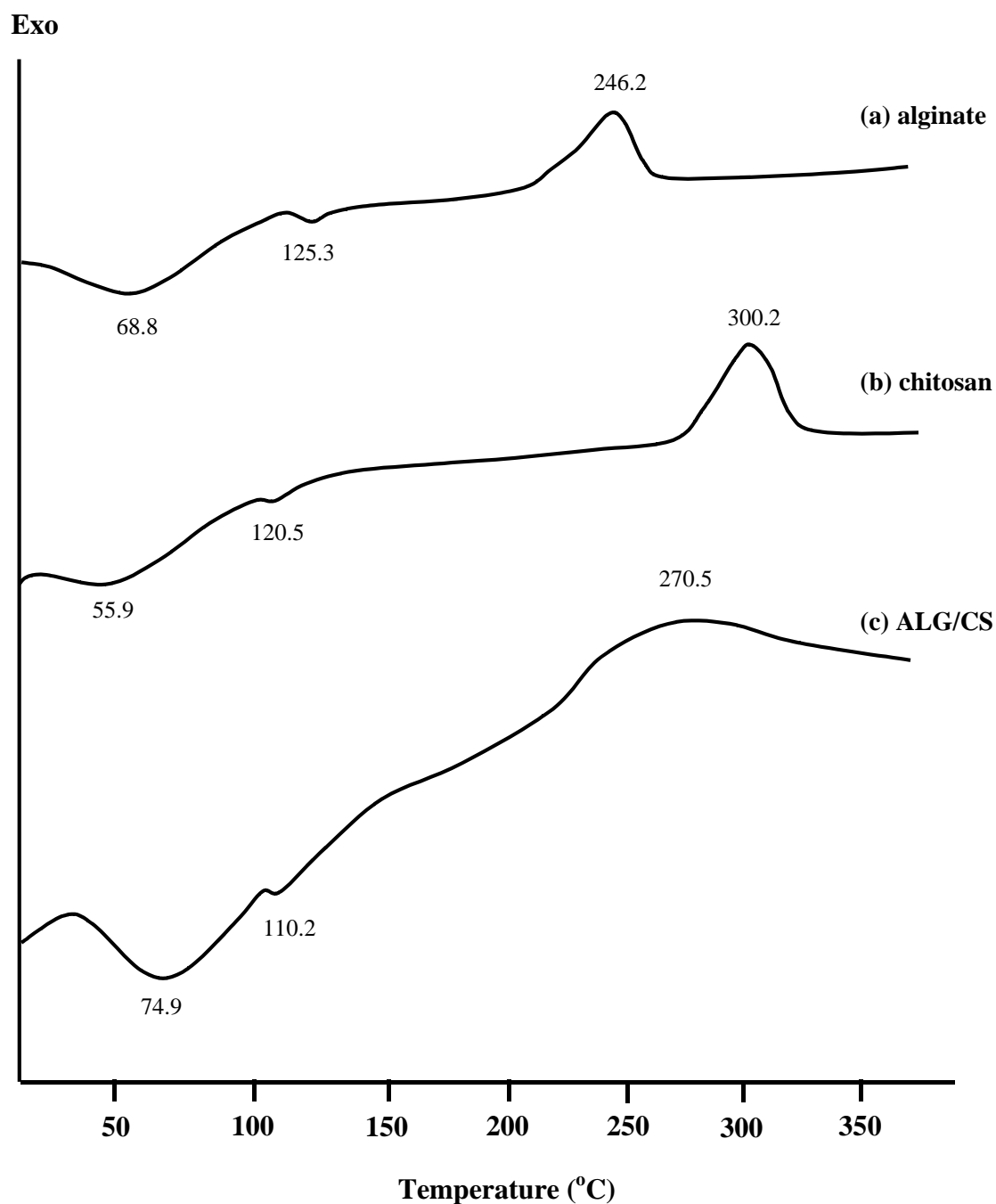


Figure 4.11 DSC thermograms of (a) alginate (b) chitosan (c) ALG/CS-NSs

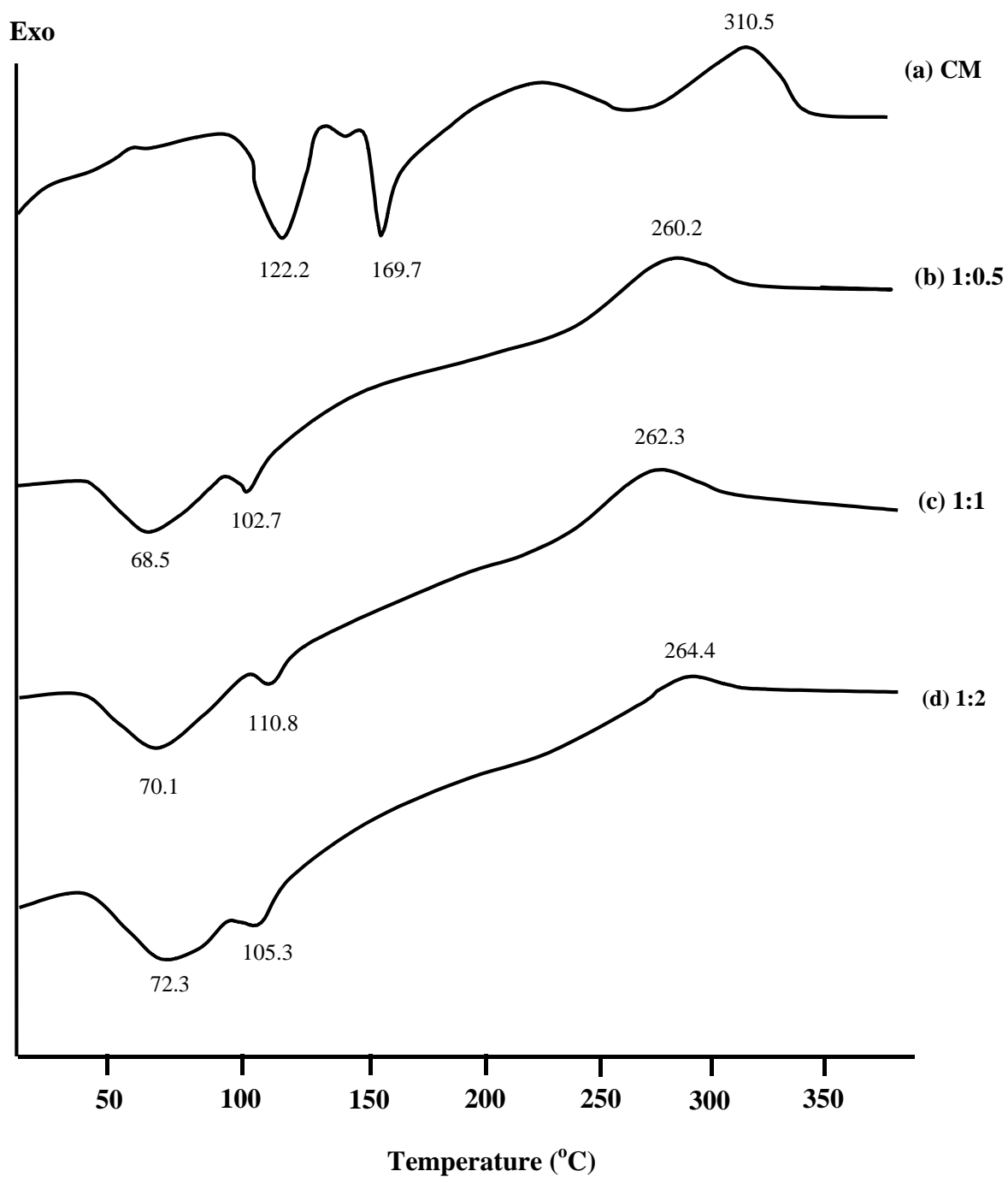


Figure 4.12 DSC thermograms of (a) clindamycin, (b) CM-ALG/CS-NSs (ALG:CM = 1:0.5), (c) CM-ALG/CS-NSs (ALG:CM = 1:1) and (d) CM-ALG/CS-NSs (ALG:CM = 1:2)

In Fig. 4.11, the thermograms of alginate (Fig. 4.11a) and chitosan (Fig. 4.11 b) showed the initial endothermic peaks at 68.8 °C and 55.9 °C and tiny endothermic peaks at 125.3, and 120.5 °C due to water loss. While exothermic peaks showed at 246.2 °C and 300.2 °C, respectively. The endothermic peaks are correlated with loss of water associated to hydrophilic group of polymer while exothermic peaks resulted from degradation of polyelectrolytes due to dehydration and depolymerization [58], [59], [60]. The thermograms of ALG/CS-NSs (Fig. 4.11c) showed the endothermic peak at 74.9 °C and water loss at 110.2 °C and the exothermic peak at 270.5 °C. It was seen that the endothermic peak was shifted to higher temperature from pure alginate and chitosan because of electrostatic interactions between anionic and cationic groups of polymer. Therefore the complexation of polyelectrolytes resulted from attraction force contributed to the shifting of higher endothermic temperature.

In Fig. 4.12, the thermograms of clindamycin (Fig. 4.12a) showed the endothermic peaks at 122.2 and 169.7 °C corresponding to the denaturation of nonstructural water and melting temperature (T_m) and the broad exothermic peak at 310.5 °C corresponded to decomposition of CM. The thermograms of CM-ALG/CS-NSs prepared at three different alginate to CM mass ratios of 1:0.5, 1:1, and 1:2 (Fig. 4.12b-d, respectively) showed the initial endothermic peaks at 70.1, 72.3, and 60.5 °C and tiny endothermic peaks at 110.8, 105.3, and 102.7 °C due to water loss. While exothermic peaks showed at 262.3, 264.4, and 260.2 °C, respectively. For all mass ratios of alginate to CM, the endothermic peaks was shifted to the lower temperature with respect to ALG/CS-NSs, because CM molecules can insert between the structure of alginate and chitosan. Therefore electrostatic interactions in nanospheres decreased, causing the temperature to shift lower. When considering the mass ratio of alginate to CM, it was observed that the thermograms of all mass ratios were similar in the shape and positions of the endothermic peaks. The DSC results showed that the interactions between ALG/CS-NSs and CM was very small and did not significantly affect their thermal properties.

4.3 Evaluation of drug content and drug encapsulation efficiency

The content of drug within CM-ALG/CS-NSs was analyzed using HPLC. The CM content was determined from the supernatant. The CM content and encapsulation efficiency were shown in Table 4.6

Table 4.6 Clindamycin content and encapsulation efficiency (%EE) of the spheres containing different alginate to drug mass ratios

Ratios of ALG:CM (w/w)	Clindamycin content (mg/mg of CM-ALG/CS-NSs)		%EE
	Theoretical	Experimental	
1:0.5	25	20.70 ± 0.11	83 ± 0.44
1:1	50	34.44 ± 1.80	69 ± 3.60
1:2	100	71.35 ± 1.91	71 ± 1.91

The CM content within CM-ALG/CS-NSs was found to increase with the increasing the amount of CM loaded. The content of CM in these spheres were 20.70, 34.44, and 71.35mg/mg of CM-ALG/CS-NSs for alginate to CM mass ratio of 1:0.5, 1:1, and 1:2 respectively. The encapsulation efficiencies were 83, 69 and 71% for alginate to CM mass ratio of 1:0.5, 1:1 and 1:2 respectively. It seemed that as the feed of CM content increased, %EE somewhat decreased. It was possible that the feed of CM content for 100 mg/mg CM-ALG/CS-NS was approaching the saturated amount in the ALG/CS matrix.

4.4 Drug release study of CM-ALG/CS-NSs in phosphate buffer medium

The content of clindamycin in CM-ALG/CS-NSs was determined by using HPLC. The cumulative drug release from ALG/CS-NSs having different drug contents were plotted as a function of time. The results indicated that the amount of drug release was increased with increasing the drug to alginate mass ratio (Fig. 4.13 and Appendix C). The cumulative amounts of drug release from CM-ALG/CS-NSs during the period of 12 h were 14.56, 18.00, and 43.63 mg/mg of CM-ALG/CS-NSs for ALG:CM mass ratios of 1:0.5, 1:1, and 1:2 respectively.

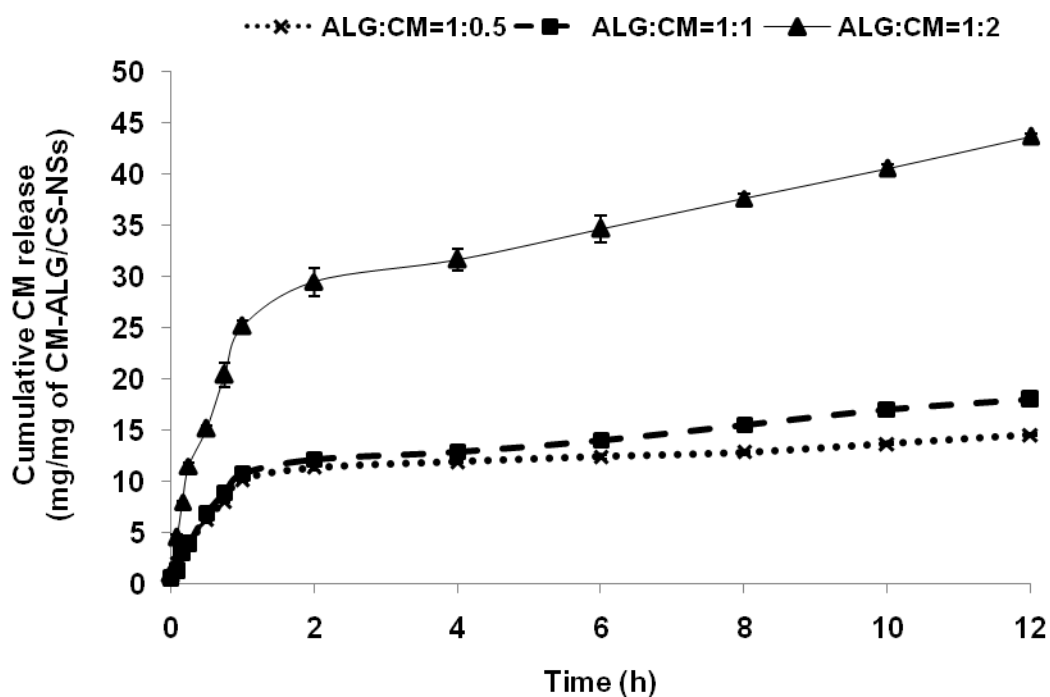


Figure 4.13 Comparison of cumulative CM release of CM-ALG/CS-NSs having different alginate to drug ratio. Error bars indicate the range of experimental reading obtained (sample number, $n = 3$)

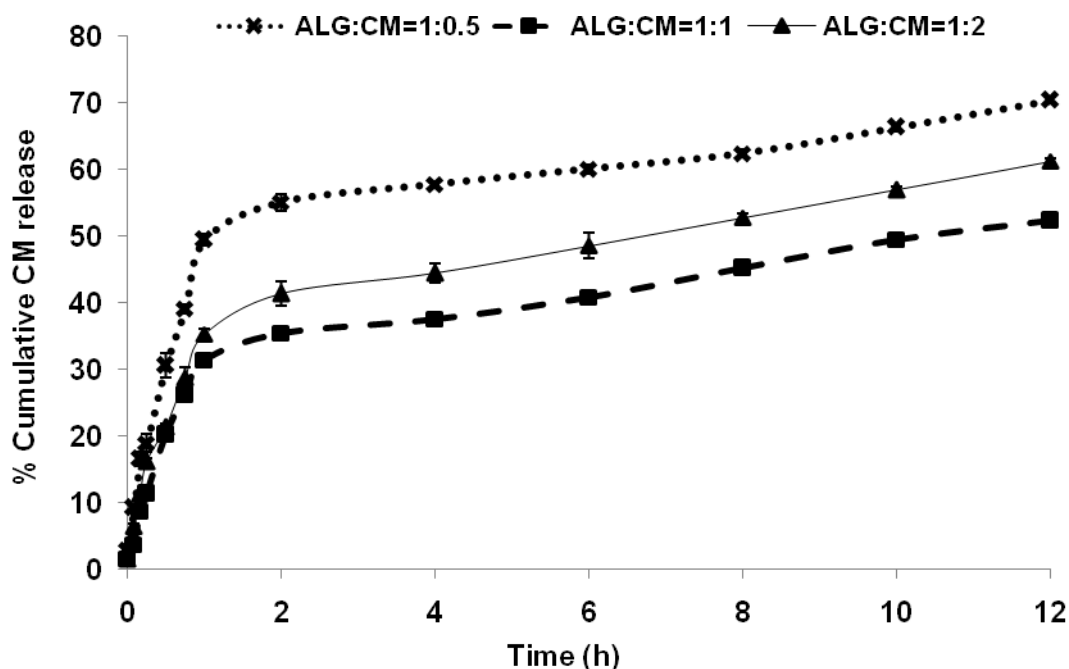


Figure 4.14 Comparison of %cumulative CM release of CM-ALG/CS-NSs having different alginate to drug ratio. Error bars indicate the range of experimental reading obtained (sample number, $n = 3$)

The percentage of cumulative CM release from CM-ALG/CS-NSs with different alginate to CM mass ratio were compared in Fig. 4.14 (Appendix C). In case of ALG:CM = 1:0.5, the result showed that about 50% of drug was released in 1 h and reached to 55% before the plateau within the period of 2 h. the cumulative release of ALG:CS = 1:1 reached to 35% during 2 h and about 50% of the drug was released in 12 h. At the same time, the cumulative drug release of ALG:CM = 1:2 reached to 40% during 2 h and about 50% of drug was released in 8 h. The result was suggests that clindamycin release *in vitro* showed a rapid initial burst, followed by constant drug release for a period of 12 h. The burst release of drug was associated with the molecules close to the nanosphere surface, which easily diffused in the initial incubation time. The dissolution process suggests that the release medium penetrates into the particles due to the hydrophilic nature of chitosan, and dissolves the entrapped clindamycin [16]. It has been previously reported that the drug release from polymeric microspheres involves two different mechanisms of drug molecules

diffusion and polymer matrix degradation [17]. Moreover, the initial burst release may be useful for the rapid control of bacterial infection [19].

4.5 *In vitro* study of clindamycin permeation through cellulose membrane

The *in vitro* cellulose membrane permeation profiles of CM are showed in Fig 4.15. In this study, ALG:CM mass ratios were varies as 1:0.5, 1:1, and 1:2. The *in vitro* permeation of CM through cellulose membrane from CM-ALG/CS-NSs was calculated in term of mean cumulative amount of permeated drug through a unit area of membrane (Q_p) at each sampling time point for a total of 12 h. In each sample, the Q_p within 12 h of incubation increased with time, indicating that CM was continuously released from the spheres and permeated through the cellulose membrane to accumulate in the buffer. The relationship between time and amount of drug permeating through the cellulose membrane (Q_p) as well as flux values are presented in Table 4.14. The permeation behaviors of CM-ALG/CS-NSs mass ratio of 1:0.5, 1:1, and 1:2 were found to be in linear relationship with time ($r^2 = 0.9524$, 0.9586 and 0.9814, respectively). The linear relationship suggests that there is a continuous release of CM from the CM-ALG/CS-NSs, resulting in continuous drug permeation through the membrane in the 12 h period. Higher drug content in the CM-ALG/CS-NSs therefore led to higher permeating flux (202.47 $\mu\text{g}/\text{cm}^2\text{h}$ for 1:0.5, 322.77 $\mu\text{g}/\text{cm}^2\text{h}$ for 1:1 and 403.62 $\mu\text{g}/\text{cm}^2\text{h}$ for 1:2 ALG:CM mass ratio). In case of the Q_p of pure CM, which was applied once on the cellulose membrane, remained almost constant throughout 12 h. This suggested that almost all of the CM permeated once through the cellulose membrane at the beginning of the experiment.

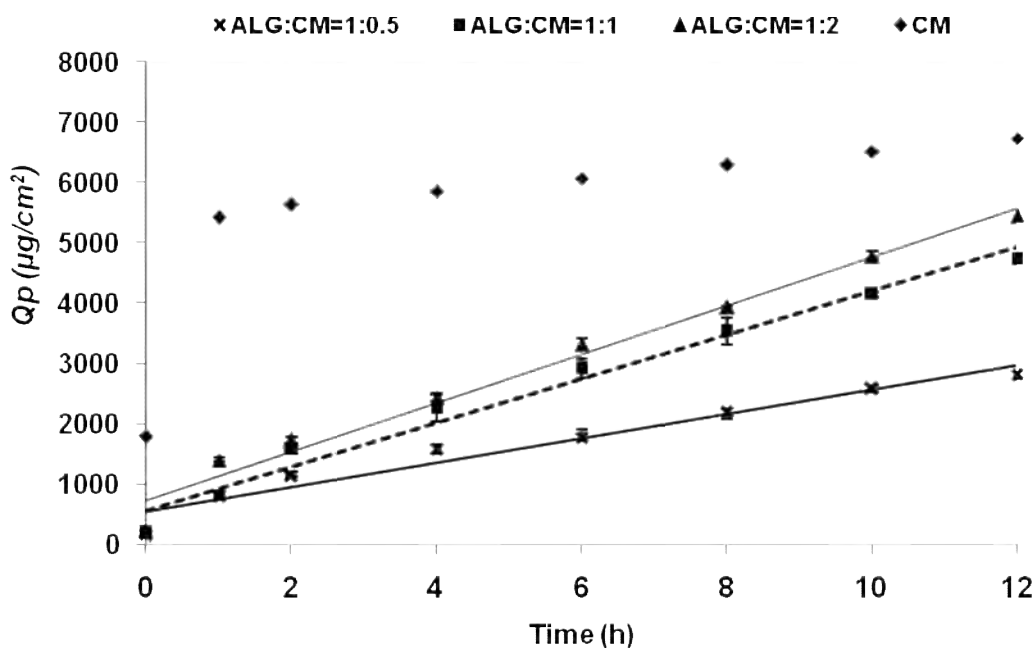


Figure 4.15 Permeation profiles of drug through cellulose membrane at various alginate to CM ratio

Table 4.7 Linear relation between amount of drug permeating through one area division of cellulose membrane (Q_p) and time

Ratio of ALG:CM	Linear relationship	r^2	F ($\mu\text{g}/\text{cm}^2\cdot\text{h}$)
1:0.5	$Q_p = 202.47t + 550.37$	0.9524	202.47
1:1	$Q_p = 322.77t + 655.04$	0.9586	322.77
1:2	$Q_p = 403.62t + 746.09$	0.9814	403.62
Pure CM	Non linear relation	0.5146	-

4.6 Antibacterial activity of CM-ALG/CS-NSs

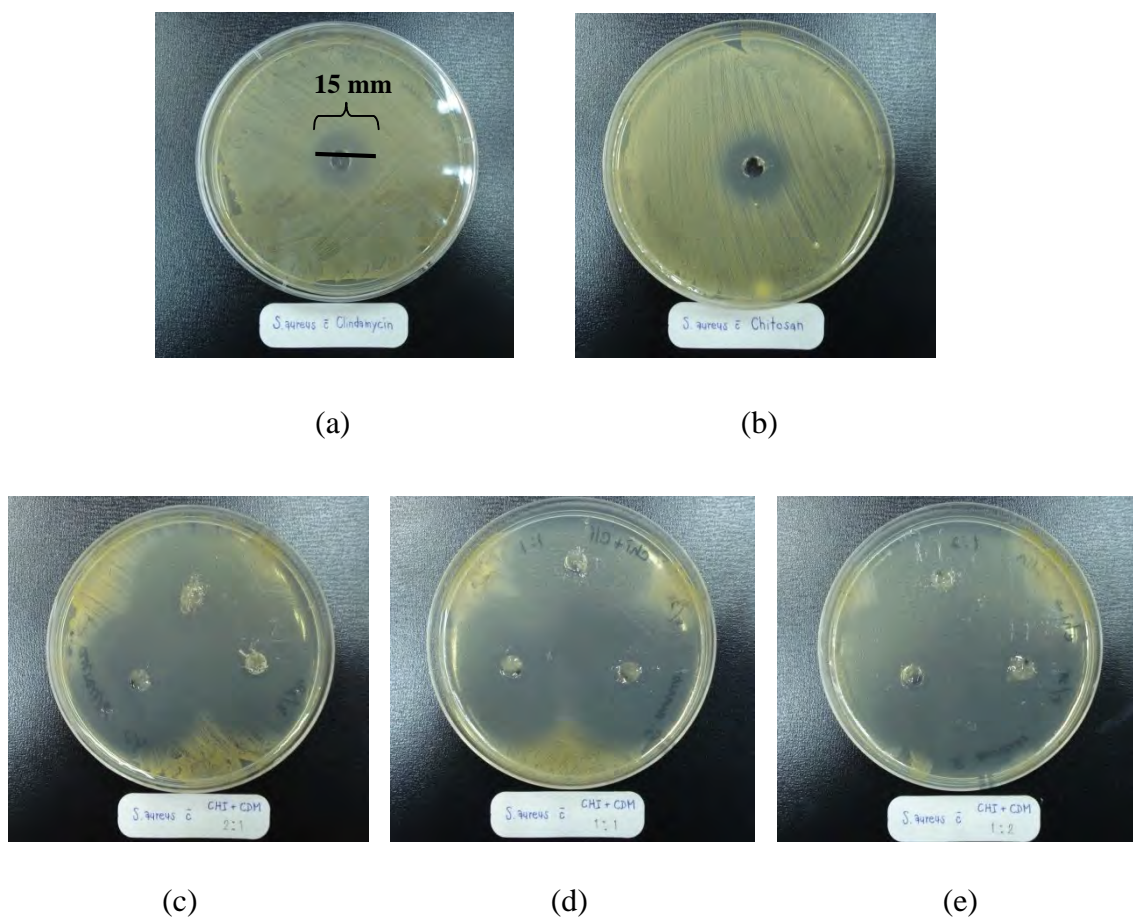


Figure 4.16 Antibacterial activity of (a) clindamycin, (b) ALG/CS, (c) ALG:CM 1:0.5, (d) ALG:CM 1:1, and (e) ALG:CM 1:2

Antibacterial activity of CM-ALG/CS-NSs were investigated by measuring inhibition zone (Fig. 4.16). A zone of inhibition of 15 mm was obtained in the plate incubated with pure clindamycin at $LC_{50} = 0.032 \mu\text{g/ml}$ (Fig. 4.16a). A zone of inhibition of 17 mm in diameter was obtained in the plate incubated with ALG/CS-NSs (Fig. 4.16b). The inhibition zone of ALG:CS mass ratio, 1:0.5, 1:1, and 1:2 was 41, 42, and 45 mm in diameter, respectively (Fig. 4.16c-e). It could be imply that clindamycin and ALG/CS-NSS have antibacterial properties. When the drug loaded within nanospheres, it also can be antibacterial. It could be suggest that there was no changes in the structure of CM within ALG/CS-NSs.

CHAPTER V

CONCLUSION

The results of this study demonstrated that the electro spraying process is a facile technique for the production of alginate/chitosan nanospheres and that the morphology and size of these spheres can be manipulated by controlling the parameters such as voltage, flow rate, needle gauge and working distance. The sphere size depended on these parameters, When increasing voltage, The sphere size was decreased whereas when increasing flow rate, needle gauge and working distance, the sphere size were increased. The optimized values for producing the clindamycin-alginate/chitosan nanosphere were as follows: voltage of 15 kv, flow rate of 10 ml/h, needle gauge of 26g and working distance of 8 cm. The average size was 855 nm measured by particle sizer and 212 nm measured by SEM.

Clindamycin-loaded alginate/chitosan nanoparticles containing different alginate to drug mass ratios (1:0.5, 1:1, and 1:2) were average particle size of 1000, 1013 and 1018 nm. The zeta potential were -54, -46 and -49 mV, respectively but not statistically significant. The clindamycin content within CM-ALG/CS-NSs was increased with the increasing alginate to drug ratio. The encapsulation efficiency of ALG:CM 1:0.5, 1:1 and 1:2 were 83, 69, 71%, respectively. The CM-ALG/CS-NSs showed a sustained release over a period of 12 h. and the clindamycin release from ALG/CS-NSs permeated through cellulose membrane over the period of 12 h.

The nanospheres formed by electro spraying contained active drug as demonstrated by the zone of inhibition on *S. aureus*. The CM-ALG/CS-NSs have an antibacterial activity when compared with pure clindamycin. Thus, the electro spraying technique could be a promising technique for the fabrication of nanoparticle-based drug delivery systems.

REFERENCES

- [1] Rumsfield, J. A. and West, D. P. Common skin disorders: Acne and psoriasis. In DiPiro, J. T., Talbert, R. L., Hayes, P. E., Yee, G. C., Matzke, G. R., Posey, L.M. (Eds.), *Pharmacotherapy, a Pathophysiologic Approach*, 2nd ed., Elsevier, Amsterdam, 1992, pp. 1387-1403.
- [2] Parry, M. F. and Rha, C. K. Pseudomembranous colitis caused by topical clindamycin phosphate. *Archives Dermatology* 122(1986): 583-594.
- [3] Honzak, L. and Sentjerc, M. Development of liposome encapsulated clindamycin for treatment of acne vulgaris. *Pflügers Archiv European Journal of Physiology* 440(2000): r044-r045.
- [4] Puttipatkhachorn, S. and Saraya S. Use of N-O Carboxymethyl chitosan in clindamycin gel for activity improvement against propionibacterium acnes. Proceedings of the Second Asia-Pacific Symposium on Chitin and Chitosan, Bangkok: Asian Institute of Technology, 21-23 November 1996. (1996): 286-290.
- [5] Sæther, H. V., Holme, H. K., Maurstad, G., Smidsrød, O. and Stokke, B. R. T. Polyelectrolyte complex formation using alginate and chitosan. *Carbohydrate Polymers* 74(2008): 813-821.
- [6] De, S. and Robinson, D. Polymer relationships during preparation of chitosan-alginate and poly-l-lysine-alginate nanospheres. *Journal of Controlled Release* 89(2003): 101-112.

- [7] Sezer, A. D. and Akbug, J. Release characteristics of chitosan treated alginate beads: I. Sustained release of a macromolecular drug from chitosan treated alginate beads. Journal of Microencapsulation 16(1999):195-203.
- [8] Liu, P. and Krishnan, T. R. Alginate-pectin-poly-L-lysine particulate as a potential controlled release formulation. Journal of Pharmacy Pharmacology 51(1999): 141-149.
- [9] Bodmeier, R. and Wang J. Microencapsulation of drugs with aqueous colloidal polymer dispersions. Journal of Pharmaceutical Sciences 82(1993): 191-194.
- [10] Guörsoy, A., Kalkan, F. and Okar, I. Preparation and tableting of dipyridamole alginate-Eudragit microspheres. Journal of Microencapsulation 15(1998): 621-628.
- [11] Chan, L. W. and Heng, P. W. S. Effects of aldehydes and methods of cross-linking on properties of calcium alginate microspheres prepared by emulsification. Biomaterials 23(2002): 1319-1326.
- [12] Kulkarni, A. R., Soppimath, K. S., Aralaguppi, M. I., Aminabhavi, T. M. and Rudzinski, W. E. Preparation of cross-linked sodium alginate microparticles using glutaraldehyde in methanol. Drug Development and Industrial Pharmacy. 26 (2000): 1121-1124.
- [13] Kulkarni, A. R., Soppimath, K. S., Aminabhavi, T. M., Dave, A. M. and M. H. Metha. Glutaraldehyde cross-linked sodium alginate beads containing liquid pesticide for soil application. Journal of Controlled Release 63(2000): 97-105.

- [14] Ferreira, A. P. and Almeida, A. J. Cross-linked alginate-gelatin beads: a new matrix for controlled release of pindolol. Journal of Controlled Release 97(2004): 431-439.
- [15] Lertsutthiwong, P., Rojsitthisak, P. and Nimmannit, U. Preparation of turmeric oil-loaded chitosan-alginate biopolymeric nanocapsules. Materials Science and Engineering 29(2009): 856-860.
- [16] Sarmiento, B., Ferreira, D., Veiga, F. and Ribeiro, A. N. Characterization of insulin-loaded alginate nanoparticles produced by ionotropic pre-gelation through DSC and FTIR studies. Carbohydrate Polymers 66(2006): 1-7.
- [17] Silva, C., Ribeiro, A., Figueiredo, M., Ferreira, D. and Veiga, F. Microencapsulation of hemoglobin in chitosan-coated alginate microspheres prepared by emulsification/internal gelation. The AAPS Journal 7(2005): E903-E913.
- [18] Jaworek, A. and Sobczyk, A. T. Electro spraying route to nanotechnology: An overview. Journal of Electrostatics 66(2008): 197-219.
- [19] Jaworek, A. Micro- and nanoparticle production by electro spraying. Powder Technology 176(2007): 18-35.
- [20] Arya, N., Chakraborty, S., Dube, N. and Katti, D. S. Electro spraying: A facile technique for synthesis of chitosan-based micro/nanospheres for drug delivery applications. Journal of Biomedical Materials Research Part B: Applied Biomaterials 88(2009): 17-31
- [21] Xie, J. and Wang, C. H. Electro spray in the dripping mode for cell microencapsulation. Journal of Colloid and Interface Science 312(2007): 247-255.

- [22] Sasaki, E., Kurayama, F., Ida, J. I., Matsuyama, T. and Yamamoto, H. Preparation of microcapsules by electrostatic atomization. Journal of Electrostatics 66(2008): 312-318.
- [23] Xu, Y., and Hanna M. A. Electrospayed bovine serum albumin-loaded tripolyphosphate cross-linked chitosan capsules: Synthesis and characterization. Journal of Microencapsulation 24(2007): 143-151.
- [24] Moltugh, D. J. A guide to the seaweed industry (Rome: FAO, 2003)
- [25] Ravi Kumar, M. N. V. A review of chitin and chitosan applications. Reactive and Functional Polymers 46(2000): 1-27.
- [26] Available from: <http://www.france-chitine.com/util.e.html>
- [27] Whitehead, L., Collett, J. H. and Fell, J. T. Amoxicillin release from a floating dosage form based on alginates. International Journal of Pharmaceutics 210(2000): 51-59.
- [28] Sriamornsak, P. Effect of calcium concentration, hardening agent and drying condition on release characteristics of oral protein from calcium pectinate gel beads. European Journal of Pharmaceutical Sciences 8(1999): 221-227.
- [29] Tapia, C., Escobar, Z., Costa, E., Sapag-Hagar, J., Valenzuela, F., Basualto, C., Nella Gai, M. and Yazdani-Pedram, M. Comparative studies on polyelectrolyte complexes and mixtures of chitosan-alginate and chitosan-carrageenan as prolonged diltiazem clorhydrate release systems. European Journal of Pharmaceutics and Biopharmaceutics 57(2004): 65-75.
- [30] Hoffman, A. S. Hydrogels for biomedical applications. Advanced Drug Delivery Reviews 54 (2003): 3-12.
- [31] Holly, A. and Stevens, M. D. Clindamycin. 4(1997): 251-253.

- [32] Available from: <http://www.clindamycin.wikipedia.com>
- [33] Salata, O. V. Tools of nanotechnology: electrospray. Current Nanoscience 1(2005): 25-33.
- [34] Kruis, F. E., Fissan, H., and Peled A. Synthesis of nanoparticles in the gas phase for electronic, optical and magnetic applications. A review Journal of Aerosol Science 29(1998): 511-535.
- [35] Shorey, J. D. and Michelson, D. On the mechanism of electrospraying. Nuclear Instrument and Methods 82(1970): 295-296.
- [36] Baldwin, S. P. and Saltzman, W. M. Materials for protein delivery in tissue engineering. Advanced Drug Delivery Reviews 33(1998): 71-86.
- [37] Available from: <http://www.devicelink.com/mpb/archive/97/11/003.html> [1997]
- [38] Advances in Controlled Release Technology: Polymeric Delivery Systems for Pharmaceuticals, Proteins and Other Agents. Available from: http://web.mit.edu/mitpep/pi/courses/controlled_release_technology.html [2008, July 21-25]
- [39] Bosman, Ingrid J., Ensing, K. and Zeeuw, Rokus A. de. Standardization procedure for the in vitro skin permeation of anticholinergics. International Journal of Pharmaceutics 169(1998): 65-73.
- [40] Perme Gear, Inc. Equipment that measures permeation through membranes. Available from: <http://www.permegear.com/fc01.gif> [2005]
- [41] Modamio, P., Lastra, C. F., and E. L. Marino. A comparative in vitro study of percutaneous penetration of blockers in human skin. International Journal of Pharmaceutics 194(2000): 249-259.

- [42] Modamio, P., Lastra C. F. and Marino, E. L. Transdermal absorption of celiprolol and bisoprolol in human skin in vivo. International Journal of Pharmaceutics 173(1998): 141-148.
- [43] Minghetti, P., Casiraghi, A., Montanari, L. and Monzani M. V. In vitro skin permeation of sinitrodil, a member of a new class of nitrovasodilator drugs. European Journal of Pharmaceutical Sciences 7(1999): 231-236.
- [44] Puglia, C., Bonina, F., Trapani, G., Franco, M. and Ricci, M. Evaluation of in vitro percutaneous absorption of lorazepam and clonazepam from hydro-alcoholic gel formulations. International Journal of Pharmaceutics 228(2001): 79-87.
- [45] Paula, C., Gareth, W. and Charles, M. H. Triclosan: release from transdermal adhesive formulations and in vitro permeation across human epidermal membranes. International Journal of Pharmaceutics 235(2002): 229-236.
- [46] Magnuson, B. M. and Koskinen, L.O.D. In vitro percutaneous penetration of topically applied capsaicin in relation to in vivo sensation responses. International Journal of Pharmaceutics 195(2000): 55-62.
- [47] Sartorelli, P., Andersen, H. R., Angerer, J., Corish, J., Drexler, H., Goen, T., Griffin, P., Hotchkiss, S. A. M., Larese, F., Montomoli, L., Perkins, J., Schmelz, M., Sandt, J. van de, and Williams, F. Percutaneous penetration studies for risk assessment. Environment Toxicology and Pharmacology 8 (2002): 133-152.
- [48] Kimura, C., Nakanishi, T. and Tojo, K. Skin permeation of ketotifen applied from stick-type formulation. European Journal of Pharmaceutics and Biopharmaceutics 67(2007): 420-424.

- [49] Xie, Y., Xu, B., PhD. and Gao, Y. Controlled transdermal delivery of model drug compounds by MEMS microneedle array. Nanomedicine: Nanotechnology, Biology, and Medicine 1(2005): 184-190.
- [50] Ropke, C. D., Kaneko, T. M., Rodrigues, R. M., Silva, V. V. da, Barros, S., Sawada, Tania C. H., Kato, Massuo J. and Barros, Silvia B. M. Evaluation of percutaneous absorption of 4-nerolidylcatechol from four topical formulations. International Journal of Pharmaceutics 249(2002): 106-116.
- [51] Bowen, Jenna L. and Heard, Charles M. Film drying and complexation effects in the simultaneous skin permeation of ketoprofen and propylene glycol from simple gel formulations. International Journal of Pharmaceutics 307(2006): 251-257.
- [52] Kerec, M., Bogataj, M., Veranic, P. and Mrhar, A. Permeability of pig urinary bladder wall: the effect of chitosan and the role of calcium. European Journal of Pharmaceutical Sciences 25(2005): 113-121.
- [53] Ngawhirunpat, T., Opanasopit, P. and Prakongpan, S. European. Comparison of skin transport and metabolism of ethyl nicotinate in various species. Journal of Pharmaceutics and Biopharmaceutics 58(2004): 645-651.
- [54] Kang, L., Jun, H. W., and McCall, J. W. Physicochemical studies of lidocaine-menthol binary systems for enhanced membrane transport. International Journal of Pharmaceutics 206(2000): 35-42.
- [55] Ribeiro, A. J., Silva, C., Ferreira, D., & Veiga, F. Chitosan reinforced alginate microspheres obtained through the emulsification/ internal gelation technique. European Journal of Pharmaceutical Sciences 25(1)(2005): 31-40.

- [56] Kang, H. A., Shin, M. S. and Yang, J. W. Preparation and characterization of hydrophobically modified alginate. Polymer Bulletin 47(2002): 429-435.
- [57] Lin, Y. H., Mi, F. L., Chen, C.T., Chang, W. C., Peng, S. F., Liang, H. F. and Sung, H. W. Preparation and Characterization of Nanoparticles Shelled with Chitosan for Oral Insulin Delivery. Biomacromolecules 8(2006): 146-152.
- [58] Mimmo, T., Marzadori, C., Montecchio, D. and Gessa, C. Characterisation of Ca- and Al-pectate gels by thermal analysis and FT-IR spectroscopy. Carbohydrate Research 340(2005): 2510-2519.
- [59] Soares, J. P., Santos, J. E., Chierice, G. O. and Cavalheiro, E. T. G. Thermal behavior of alginic acid and its sodium salt. Ecletica Quimica 29(2004): 57-63.
- [60] Zohuriaan, M. J. and Shokrolahi, F. Thermal studies on natural and modified gums. Polymer Testing 23(2004): 575-579.

APPENDICES

Appendix A

Statistic analysis

In case of spherical size as measured by SEM

Table 1A Effect of voltage on spherical size of ALG/CS-NSs

Voltage (kV)	Mean size (nm)	Variance	N
5	921.23	17424.8453	100
10	490.53	14400.3246	100
15	211.94	643.0469	100

$$F = 1537.7835, \quad F_{\text{crit}} = 3.0261$$

$$P = 4.662 \times 10^{-57}$$

At the 0.05 level,

The three means are significantly different.

Table 2A Effect of flow rate on spherical size of ALG/CS-NSs

Flow rate (ml/h)	Mean size (nm)	Variance	N
10	211.94	643.0469	100
15	450.35	14400.3452	100
20	521.12	20449.8752	100

$$F = 837.7846, \quad F_{\text{crit}} = 3.0261$$

$$P = 7.534 \times 10^{-76}$$

At the 0.05 level,

The three means are significantly different.

Table 3A Effect of needle gauge on spherical size of ALG/CS-NSs

Needle gauge	Mean size (nm)	Variance	N
18	882.73	18225.2463	100
20	342.45	2916.5437	100
26	211.94	643.0469	100

$$F = 1727.4377, \quad F_{\text{crit}} = 3.0261$$

$$P = 2.682 \times 10^{-164}$$

At the 0.05 level,

The three means are significantly different.

Table 4A Effect of working distance on spherical size of ALG/CS-NSs

Working distance	Mean size (nm)	Variance	N
8	211.94	643.0469	100
12	303.25	2628.1692	100
15	343.16	1945.9741	100

$$F = 260.1880, \quad F_{\text{crit}} = 3.0261$$

$$P = 5.125 \times 10^{-66}$$

At the 0.05 level,

The three means are significantly different.

In case of spherical size as measured by particle sizer

Table 5A Effect of voltage on spherical size of ALG/CS-NSs

Voltage (kV)	Mean size (nm)	Variance	N
5	1219.022	137396.7169	9
10	881.3444	105114.0528	9
15	855.2778	8531.244444	9

$F = 4.4378,$ $F_{crit} = 3.4028$

$P = 0.023079$

At the 0.05 level,

The three means are significantly different.

Table 6A Effect of flow rate on spherical size of ALG/CS-NSs

Flow rate (ml/h)	Mean size (nm)	Variance	N
10	855.27778	8531.244444	9
15	959.23333	51004.7475	9
20	964.51111	25850.07361	9

$F = 1.1998,$ $F_{crit} = 3.4028$

$P = 0.318678$

At the 0.05 level,

The three means are no significantly different.

Table 7A Effect of needle gauge on spherical size of ALG/CS-NSs

Needle gauge	Mean size (nm)	Variance	N
18	1034.722	45495.85	9
20	874.3444	98884.94	9
26	855.2778	8531.244	9

$F = 1.7152$, $F_{crit} = 3.4028$

$P = 0.201248$

At the 0.05 level,

The three means are no significantly different.

Table 8A Effect of working distance on spherical size of ALG/CS-NSs

Working distance	Mean size (nm)	Variance	N
8	855.2778	8531.244	9
12	978.7889	62201.19	9
15	1143.744	269472.8	9

$F = 1.6623$, $F_{crit} = 3.4028$

$P = 0.210793$

At the 0.05 level,

The three means are no significantly different.

Appendix B

Calibration Curve

The concentration versus peak area data of CM in distilled water at 262 nm and in phosphate buffer pH 7.4 at 262 nm are presented in Table 1 and 2. They show a linear relationship with the correlation coefficient = 0.9997 and 0.9992.

Table 1B Peak area of CM in distilled water determined at 262 nm

Concentration of CM in distilled water (mg/L)	Peak area \pm SD
0	0
100	3860230 \pm 88377
200	8120564 \pm 73394
300	12545792 \pm 473469
400	16882275 \pm 408188
500	21364550 \pm 1067144
600	25474973 \pm 1041165

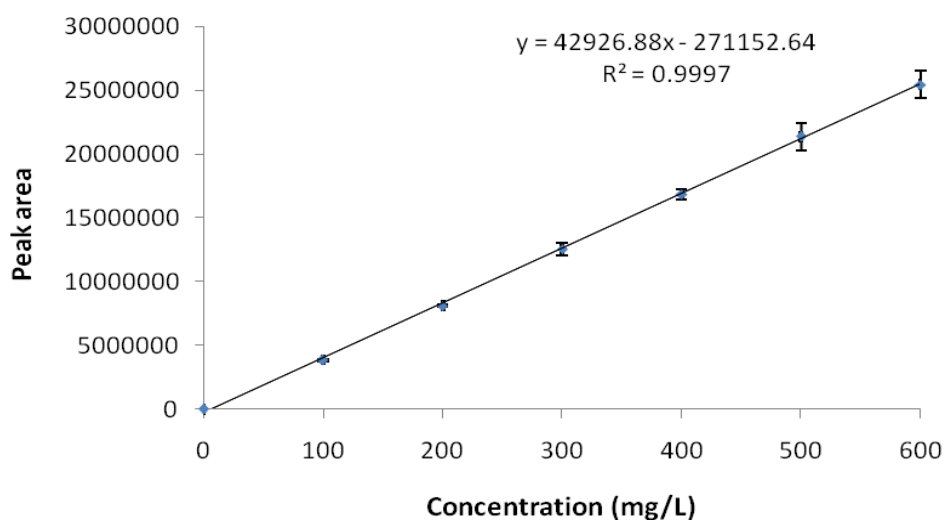


Figure 1B Standard calibration curve of peak area of CM in distilled water

$$\text{Concentration of CM solution} = \frac{\text{Peak area} + 271152.64}{42926.88} \text{ mg/L}$$

$$\begin{aligned} \text{Amount of CM (mg/mg of CM - ALG/CS- NSs)} \\ = \frac{\text{Concentration of clindamycin (mg/mL)}}{10 \text{ mg}} \times 100 \text{ mL} \end{aligned}$$

Table 2B Peak area of CM in phosphate buffer solution pH 7.4 determined at 262 nm

Concentration of CM in phosphate buffer solution pH 7.4 (mg/L)	Peak area \pm SD
0	0
100	3650689 \pm 167004
200	8004505 \pm 314875
300	12249567 \pm 372038
400	16785672 \pm 543299
500	20578632 \pm 438848

$$\text{Concentration of CM solution} = \frac{\text{Peak area} + 255858.52}{41869.48} \text{ g/mL}$$

$$\begin{aligned} \text{Amount of CM release (mg/mg of CM - ALG/CS- NSs)} \\ = \frac{\text{Concentration of clindamycin (mg/mL)}}{10 \text{ mg}} \times 100 \text{ mL} \end{aligned}$$

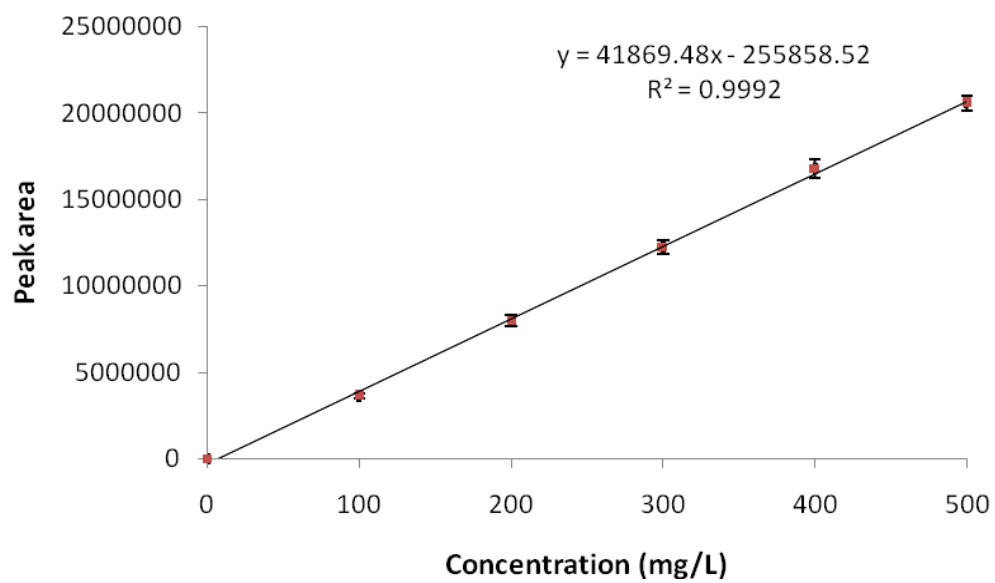


Figure 2B Standard calibration curve of peak area of CM in phosphate buffer solution pH 7.4

Appendix C

Amount of Drug Release

Table 1C Cumulative CM release from CM-ALG/CS-NSs for case of ALG:CM mass ratio = 1:0.5

Time (min)	Amount of CM release (mg/mg of CM-ALG/Cs-NSs)				
	1	2	3	Mean	SD
0	0.5764	0.5780	0.6335	0.5959	0.0325
5	1.9862	1.9098	1.8087	1.9016	0.0891
10	3.5780	3.4806	3.1661	3.4082	0.2153
15	4.2074	3.6687	3.8265	3.9009	0.2770
30	6.7519	6.1612	6.0470	6.3200	0.3783
45	8.2220	7.9521	8.0715	8.0819	0.1352
60	10.2567	10.0137	10.3829	10.2178	0.1876
120	11.6371	11.3763	11.1474	11.3869	0.2450
240	12.0465	11.9421	11.8536	11.9474	0.0965
360	12.6000	12.3491	12.3240	12.4244	0.1526
480	13.0299	12.8992	12.7822	12.9038	0.1240
600	13.6875	13.6194	13.8596	13.7221	0.1238
720	14.5898	14.4459	14.6529	14.5629	0.1061

Table 2C Cumulative CM release from CM-ALG/CS-NSs for case of ALG:CM mass ratio = 1:1

Time (min)	Amount of CM release (mg/mg of CM-ALG/Cs-NSs)				
	1	2	3	Mean	SD
0	0.5209	0.5137	0.5738	0.5362	0.0328
5	1.2700	1.2402	1.3072	1.2725	0.0336
10	3.0920	2.9367	2.9409	2.9899	0.0885
15	3.8397	3.7728	4.0606	3.8910	0.1506
30	6.9629	6.5201	7.3064	6.9298	0.3942
45	8.7607	9.2245	8.9282	8.9711	0.2349
60	11.0884	11.0712	10.2512	10.8036	0.4785
120	12.3653	12.1048	12.1301	12.2001	0.1436
240	12.8837	12.9740	12.8832	12.9136	0.0523
360	14.2846	14.2661	13.5525	14.0344	0.4174
480	15.7248	15.2382	15.6408	15.5346	0.2601
600	16.7615	17.1576	17.1785	17.0325	0.2350
720	18.2315	17.7701	17.9998	18.0004	0.2307

Table 3C Cumulative CM release from CM-ALG/CS-NSs for case of ALG:CM mass ratio = 1:2

Time (min)	Amount of CM release (mg/mg of CM-ALG/Cs-NSs)				
	1	2	3	Mean	SD
0	1.2133	0.8735	0.9798	1.0222	0.1738
5	4.2626	4.6546	4.7968	4.5713	0.2767
10	8.0173	8.0043	8.0965	8.0394	0.0499
15	11.9008	11.3910	11.1555	11.4824	0.3810
30	15.0324	15.5613	14.9785	15.1908	0.3221
45	19.9147	19.6292	21.8006	20.4482	1.1799
60	25.7802	25.0526	24.6106	25.1478	0.5906
120	28.2579	29.2324	30.9080	29.4661	1.3404
240	31.1690	30.9460	32.8425	31.6525	1.0366
360	36.1783	34.0769	33.6602	34.6385	1.3497
480	37.1609	37.7689	37.9602	37.6300	0.4173
600	40.0821	40.9574	40.6070	40.5488	0.4405
720	43.9097	43.2765	43.7133	43.6332	0.3241

Appendix D

Percentage of Cumulative Drug Release

Table 1D Percentage of CM release from CM-ALG/CS-NSs for case of ALG:CM mass ratio = 1:0.5

Time (min)	Percentage of CM Release				
	1	2	3	Mean	SD
0	2.78	2.79	3.06	2.88	0.16
5	9.60	9.23	8.74	9.19	0.43
10	17.29	16.81	15.30	16.46	1.04
15	20.33	17.72	18.49	18.84	1.34
30	32.62	29.76	29.21	30.53	1.83
45	39.72	38.42	38.99	39.04	0.65
60	49.55	48.38	50.16	49.36	0.91
120	56.22	54.96	53.85	55.01	1.18
240	58.20	57.69	57.26	57.72	0.47
360	60.87	59.66	59.54	60.02	0.74
480	62.95	62.31	61.75	62.34	0.60
600	66.12	65.79	66.95	66.29	0.60
720	70.48	69.79	70.79	70.35	0.51

Table 2D Percentage of CM release from CM-ALG/CS-NSs for case of ALG:CM mass ratio = 1:1

Time (min)	Percentage of CM Release				
	1	2	3	Mean	SD
0	1.51	1.49	1.67	1.56	0.10
5	3.69	3.60	3.80	3.69	0.10
10	8.98	8.53	8.54	8.68	0.26
15	11.15	10.95	11.79	11.30	0.44
30	20.22	18.93	21.21	20.12	1.14
45	25.44	26.78	25.92	26.05	0.68
60	32.20	32.15	29.77	31.37	1.39
120	35.90	35.15	35.22	35.42	0.42
240	37.41	37.67	37.41	37.50	0.15
360	41.48	41.42	39.35	40.75	1.21
480	45.66	44.25	45.41	45.11	0.76
600	48.67	49.82	49.88	49.46	0.68
720	52.94	51.60	52.26	52.27	0.67

Table 3D Percentage of CM release from CM-ALG/CS-NSs for case of ALG:CM mass ratio = 1:2

Time (min)	Percentage of CM Release				
	1	2	3	Mean	SD
0	1.70	1.22	1.37	1.43	0.24
5	5.97	6.52	6.72	6.41	0.39
10	11.24	11.22	11.35	11.27	0.07
15	16.68	15.96	15.63	16.09	0.53
30	21.07	21.81	20.99	21.29	0.45
45	27.91	27.51	30.55	28.66	1.65
60	36.13	35.11	34.49	35.25	0.83
120	39.60	40.97	43.32	41.30	1.88
240	43.68	43.37	46.03	44.36	1.45
360	50.71	47.76	47.18	48.55	1.89
480	52.08	52.93	53.20	52.74	0.58
600	56.18	57.40	56.91	56.83	0.62
720	61.54	60.65	61.27	61.15	0.45

Appendix E

In Vitro Membrane Permeation

Table 1E Cumulative amount of permeated drug through a unit area of cellulose membrane (Q_p), $\mu\text{g}/\text{cm}^2$ for case of CM-ALG/CS-NSs mass ratio = 1:0.5

Time (hour)	Q_p (1)	Q_p (2)	Q_p (3)	Mean	SD
0	164.88	162.42	163.60	163.63	1.23
1	768.11	829.00	785.51	794.21	31.37
2	1131.06	1148.81	1178.96	1152.94	24.22
4	1615.84	1656.57	1514.13	1595.51	73.36
6	1797.85	1718.68	1845.98	1787.50	64.28
8	2341.58	2215.86	2091.80	2216.41	124.89
10	2621.45	2540.40	2575.76	2579.20	40.63
12	2805.31	2888.57	2765.25	2819.71	62.91

Table 2E Cumulative amount of permeated drug through a unit area of cellulose membrane (Q_p), $\mu\text{g}/\text{cm}^2$ for case of CM-ALG/CS-NSs mass ratio = 1:1

Time (hour)	Q_p (1)	Q_p (2)	Q_p (3)	Mean	SD
0	198.01	199.83	204.68	200.84	3.45
1	853.52	839.52	773.44	822.16	42.77
2	1637.62	1594.20	1508.26	1580.03	65.83
4	2426.47	2372.53	2009.36	2269.45	226.86
6	3061.70	2952.17	2750.86	2921.58	157.66
8	3720.70	3606.77	3290.79	3539.42	222.73
10	4115.52	4151.66	4183.04	4150.07	33.79
12	4683.50	4732.61	4848.71	4754.94	84.84

Table 3E Cumulative amount of permeated drug through a unit area of cellulose membrane (Q_p), $\mu\text{g}/\text{cm}^2$ for case of CM-ALG/CS-NSs mass ratio = 1:2

Time (hour)	Q_p (1)	Q_p (2)	Q_p (3)	Mean	SD
0	252.07	238.84	212.62	234.51	20.08
1	1410.98	1416.20	1395.17	1407.45	10.95
2	1697.17	1713.26	1776.60	1729.01	41.99
4	2372.23	2467.95	2509.39	2449.85	70.35
6	3249.26	3390.85	3348.16	3329.42	72.63
8	3844.16	3965.94	4018.43	3942.84	89.40
10	4802.80	4776.00	4755.61	4778.13	23.67
12	5361.22	5457.61	5540.38	5453.07	89.67

Table 4E Cumulative amount of permeated drug through a unit area of cellulose membrane (Q_p), $\mu\text{g}/\text{cm}^2$ for case of CM

Time (hour)	Q_p (1)	Q_p (2)	Q_p (3)	Mean	SD
0	1790.36	1793.32	1815.68	1799.79	13.84
1	5428.33	5422.72	5426.07	5425.70	2.82
2	5645.87	5640.62	5643.70	5643.39	2.64
4	5864.16	5858.79	5861.69	5861.55	2.69
6	6082.97	6076.86	6080.15	6079.99	3.06
8	6303.58	6297.13	6299.60	6300.10	3.26
10	6521.49	6515.24	6518.18	6518.30	3.13
12	6739.58	6733.19	6735.88	6736.22	3.21

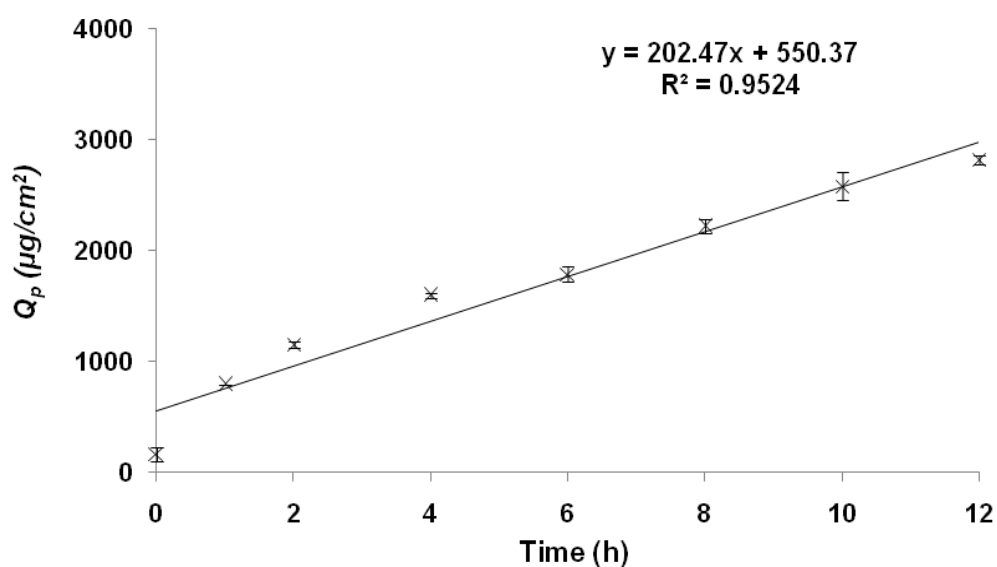


Figure 1E Permeation profiles of drug through cellulose membrane for case of CM-ALG/CS-NSs (ALG/CM mass ratio = 2:1). Q_p =Cumulative amount of permeated drug through a unit area of cellulose membrane, $\mu\text{g}/\text{cm}^2$, t =time (h). Each data represents the mean \pm SD ($n=3$).

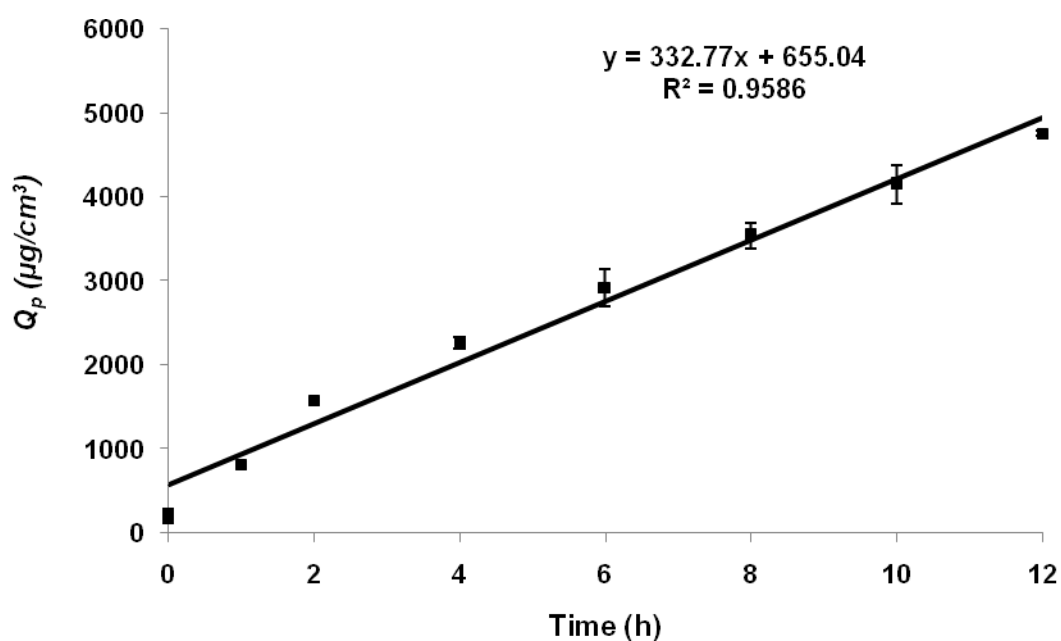


Figure 2E Permeation profiles of drug through cellulose membrane for case of CM-ALG/CS-NSs (ALG/CM mass ratio = 1:1). Q_p =Cumulative amount of permeated drug through a unit area of cellulose membrane, $\mu\text{g}/\text{cm}^2$, t =time (h). Each data represents the mean \pm SD ($n=3$).

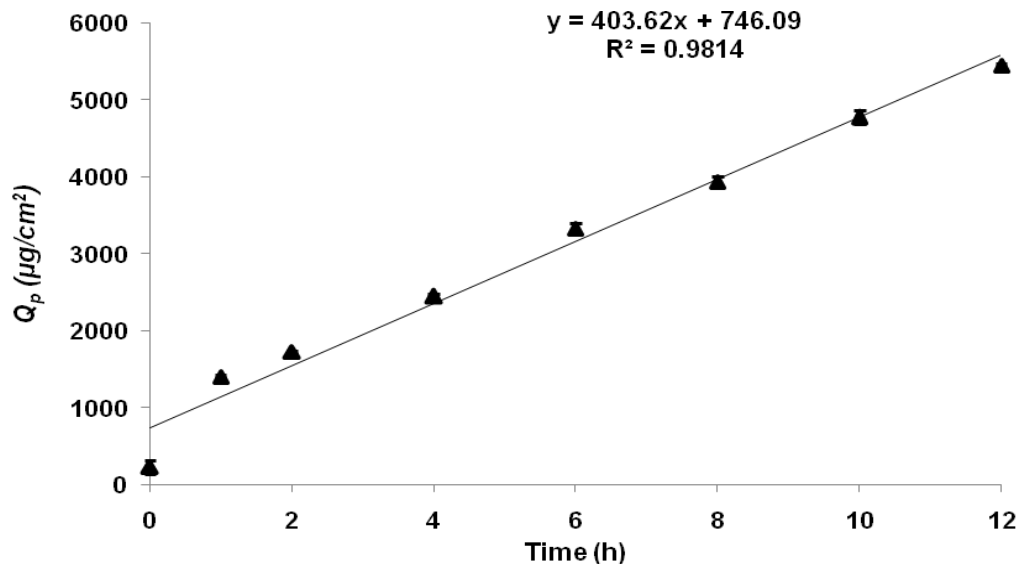


Figure 3E Permeation profiles of drug through cellulose membrane for case of CM-ALG/CS-NSs (ALG/CM mass ratio = 1:2). Q_p =Cumulative amount of permeated drug through a unit area of cellulose membrane, $\mu\text{g}/\text{cm}^2$, t =time (h). Each data represents the mean \pm SD ($n=3$).

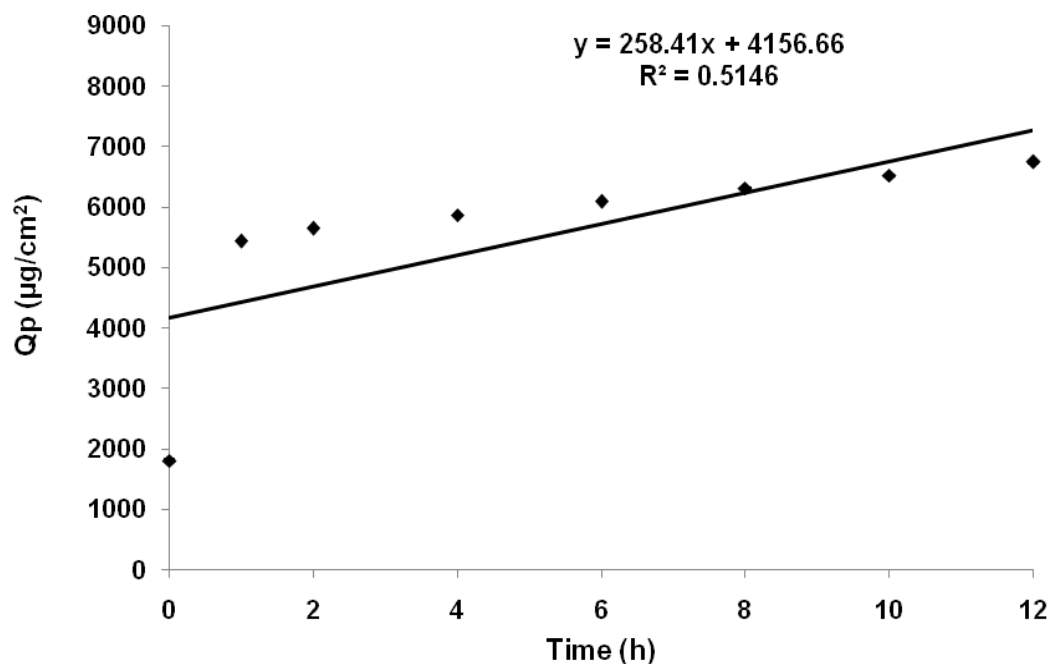


Figure 4E Permeation profiles of drug through cellulose membrane for case of CM. Q_p =Cumulative amount of permeated drug through a unit area of cellulose membrane, $\mu\text{g}/\text{cm}^2$, t =time (h). Each data represents the mean \pm SD ($n=3$).

VITAE

Name : Miss Ornuma Thimulnee

Date of birth : May 9, 1984

Nationality : Thai

Address : 491/69 Banchan, Muang District, Udonthani,
41000

University Education : Bachelor's Degree from Department of
General Science, Faculty of Arts and Science,
Kasetsart University, 2003-2006

Master's Degree from Program in
Petrochemistry and Polymer Science, Faculty of
Science, Chulalonglorn University, 2007-2009

Conference attendance: Oral presentation "Characterization and
preparation of clindamycin-loaded
alginate/chitosan core-shell nanoparticles by
electrospray technique" at The 11th International
Conference on Chitin and Chitosan & The 8th
Asia-Pacific Chitin and Chitosan Symposium
in Taipei, Taiwan